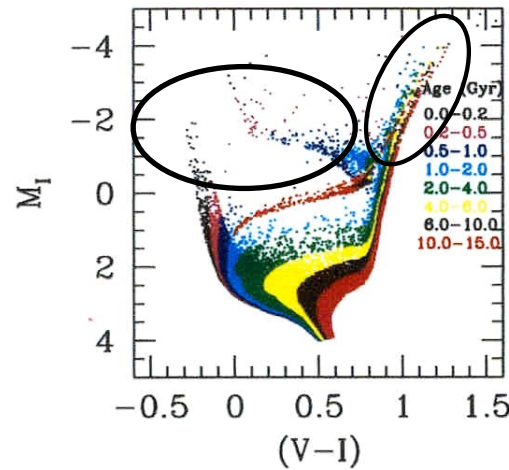


## How do we infer galaxy ages?

Closely coupled to concept of  
“stellar populations”\*

\*previously discussed in the context of colors

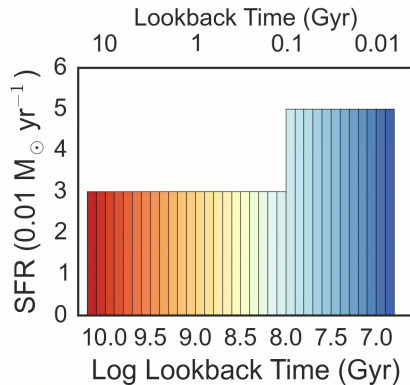
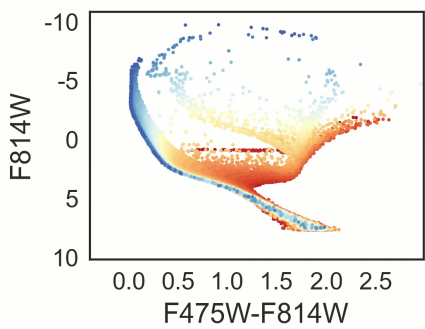
Galaxy colors/spectra are dominated by the  
brightest stars in their stellar populations



These stars are also the most massive

## Color-Magnitude Diagrams vs Time

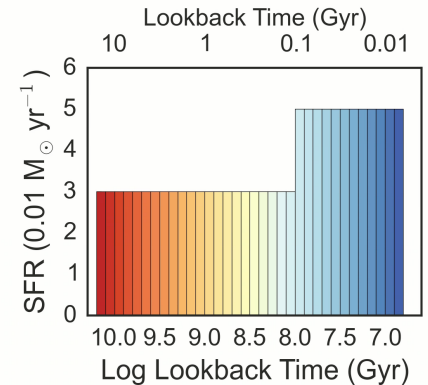
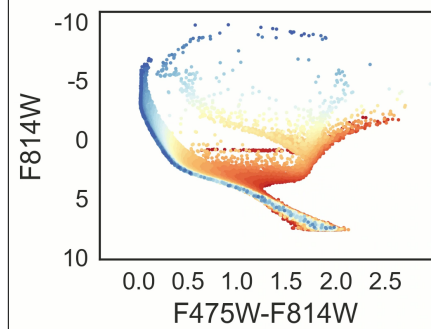
Movie Credit: Dan Weisz



What are the brightest stars at each epoch?

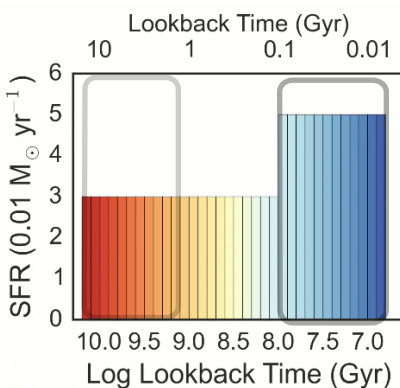
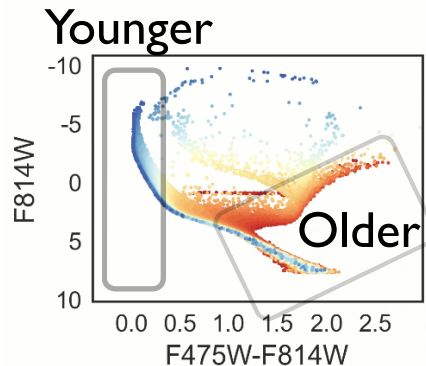
## Color-Magnitude Diagrams vs Time

Movie Credit: Dan Weisz

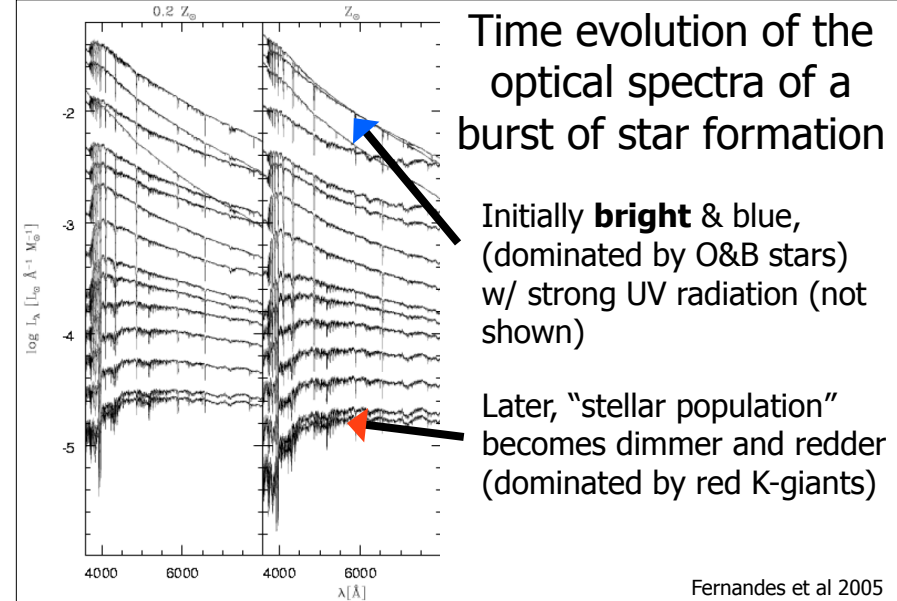


Recent SF: Bright stars are blue & luminous  
Ancient SF: Bright stars are red & dimmer

# Age resolution is $\sim$ logarithmic



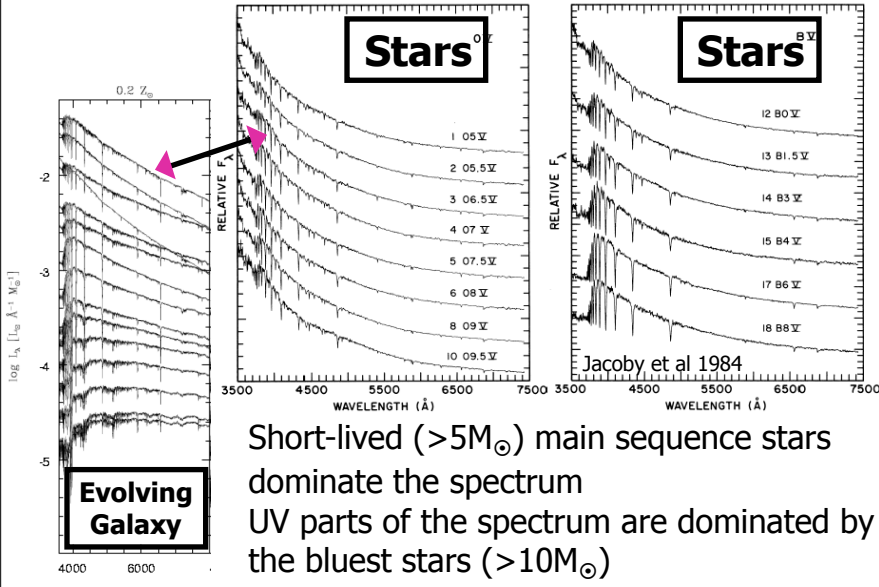
*Changes in color & luminosity:*  
Large/rapid at  $< 100$  Myr.  
Small/slow changes at  $> 2$  Gyr.



Fernandes et al 2005

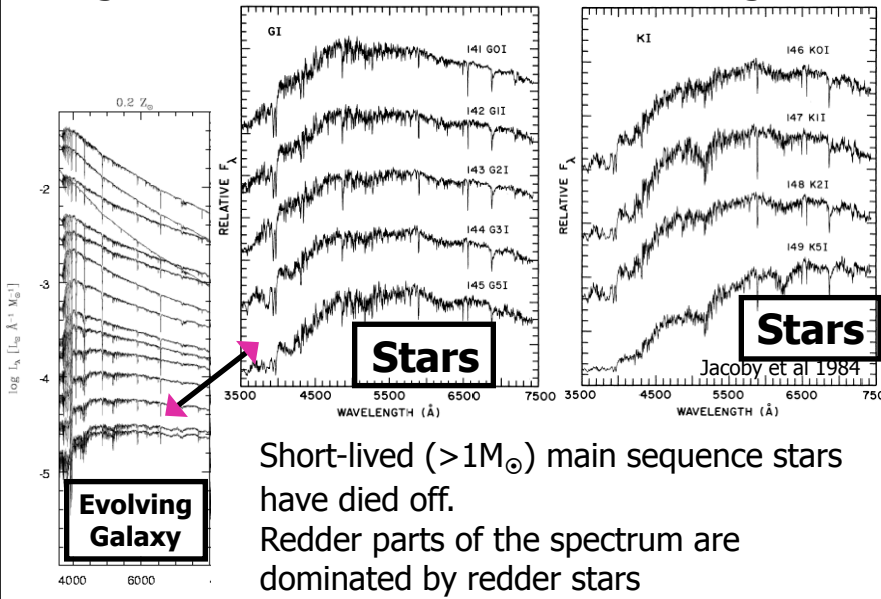
Figure 1. Spectra of the 45 SSPs used in the spectral synthesis (from BC03). The base comprises 3 different metallicities,  $Z = 0.2, 1$  and  $2.5 Z_{\odot}$ , and 15 ages: From top to bottom,  $t = 0.001, 0.00316, 0.00501, 0.01, 0.02512, 0.04, 0.10152, 0.28612, 0.64054, 0.90479, 1.434, 2.5, 5, 11$  and  $13$  Gyr. All SSPs are normalized to  $1 M_{\odot}$  at  $t = 0$ .

## A burst of SF initially looks like O & B stars



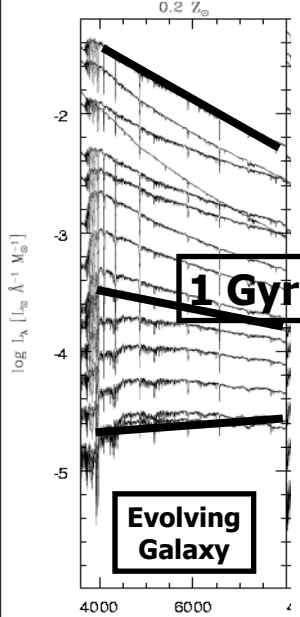
Short-lived ( $> 5 M_{\odot}$ ) main sequence stars dominate the spectrum  
UV parts of the spectrum are dominated by the bluest stars ( $> 10 M_{\odot}$ )

## Long after the burst, it looks like G/K giants



Short-lived ( $> 1 M_{\odot}$ ) main sequence stars have died off.  
Redder parts of the spectrum are dominated by redder stars

## Take-away



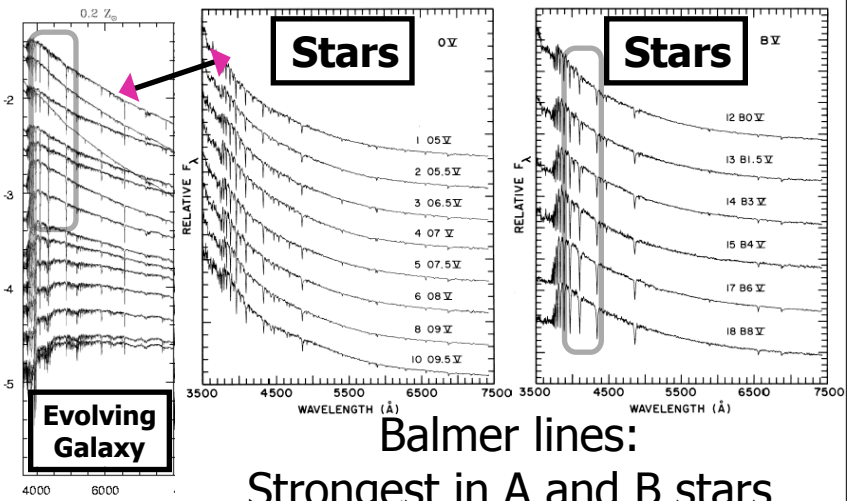
Galaxies with recent (<1Gyr) star formation will be blue

Bluer galaxies have a higher fraction of recent star formation

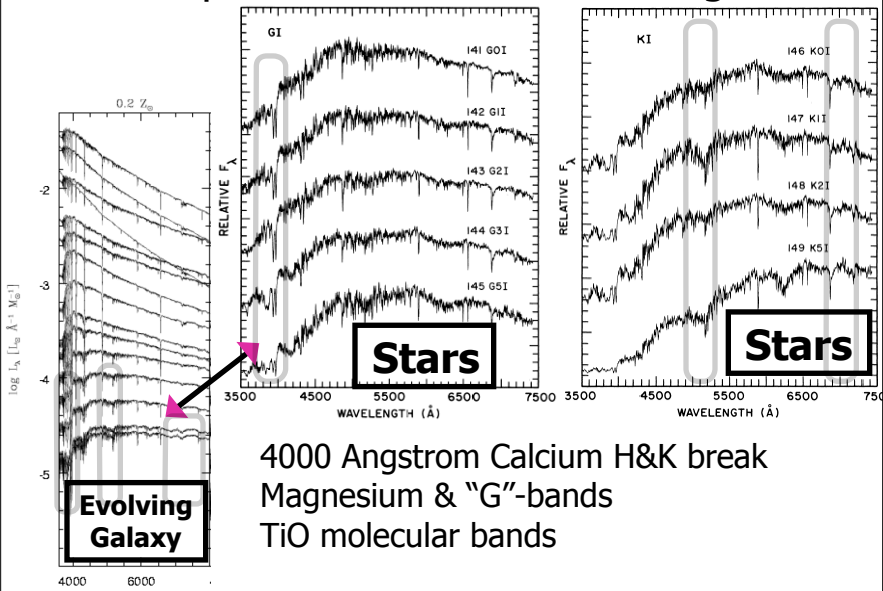
But, "blue" does not necessarily mean "currently" forming stars

Caution: Dust

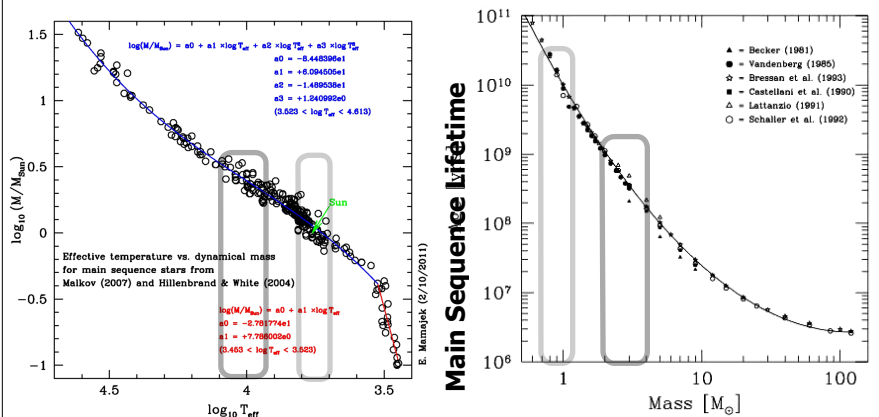
Beyond colors, use spectral features for age-dating, based on features in dominant stellar type



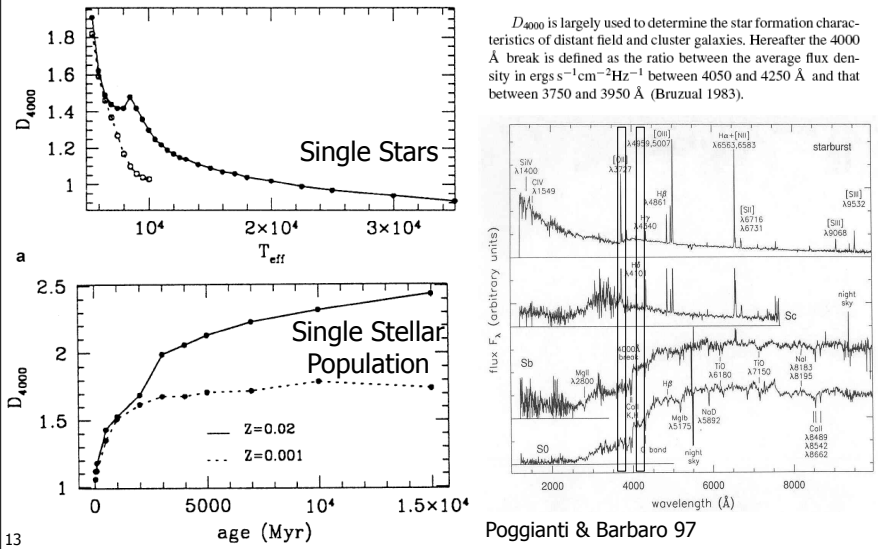
"Old" Spectral features from cool giants



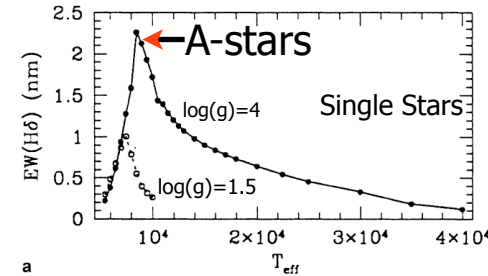
Age sensitivity comes from "what mass star is dominating spectrum"



## Ages from D<sub>4000</sub>: 4000 Angstrom Break Works to old ages, but metallicity issues



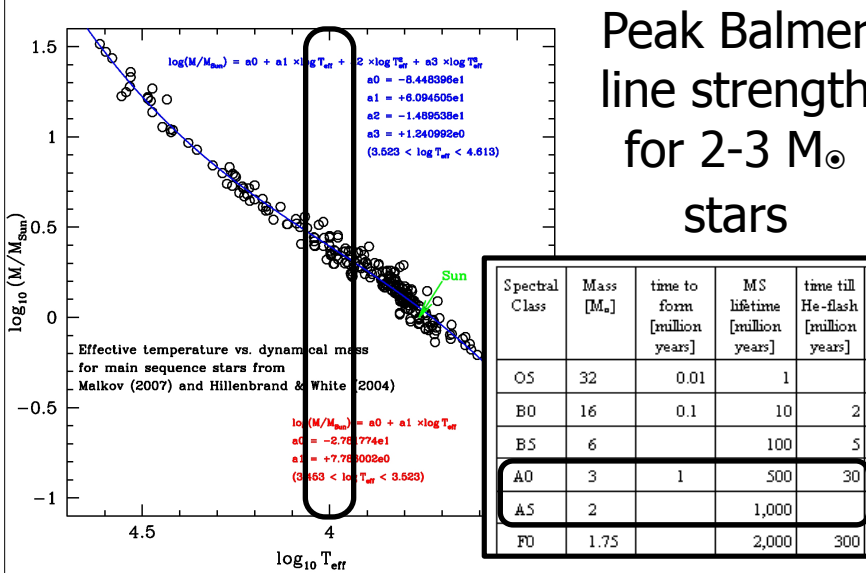
## Ages from Balmer Absorption Lines: H $\delta$



Strongest Balmer absorption lines are from A-stars with moderately high masses, and short (0.5-1 Gyr) lifetimes

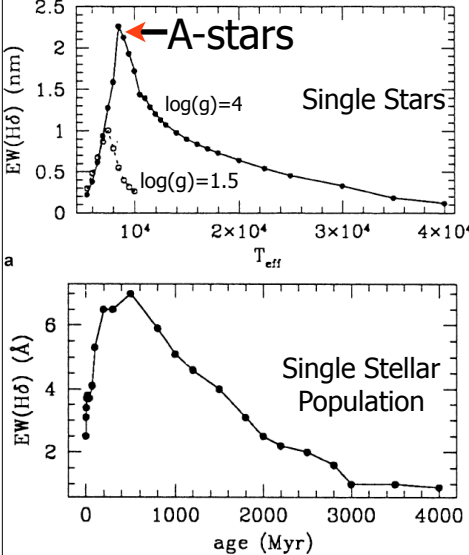
14

## Ages from Balmer Absorption Lines: H $\delta$

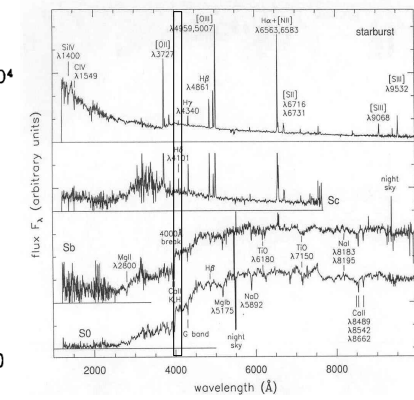


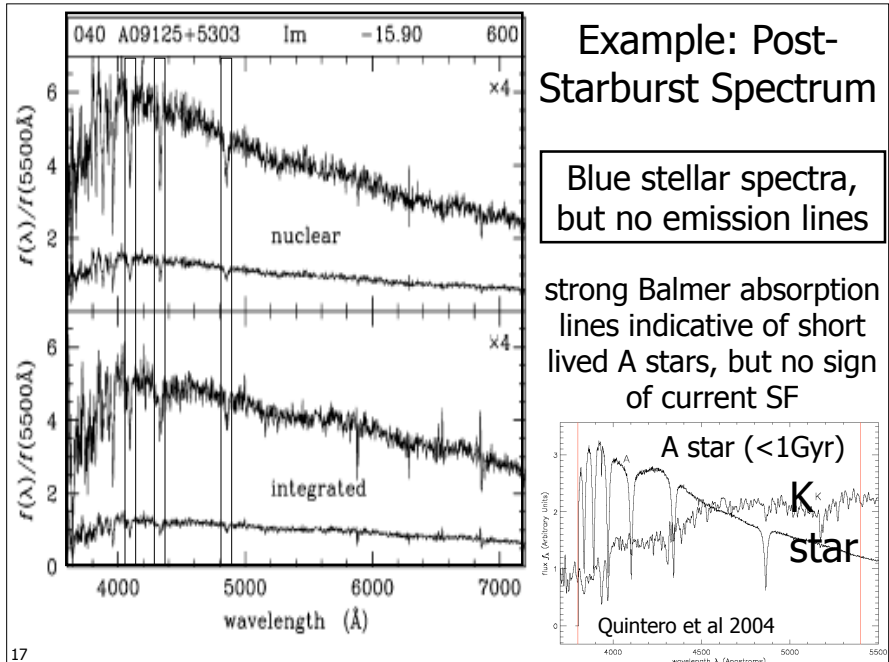
## Ages from Balmer Absorption Lines: H $\delta$

Note: Not sensitivity past a few Gyrs



16





### Example: Post- Starburst Spectrum

How do we infer star formation rates?

Similar principles apply to inferring presence of “recent” star formation

18

## Overview: Star formation in Galaxies

- Initial focus will be on global properties
  - Not concerned w/ details of how individual gas blobs turn into stars
- Measuring the “instantaneous” star formation rate (in  $M_{\odot}/\text{yr}$ )
- Variation in SFR within the galaxy population
- Correlation between physical properties & galaxy’s global star formation rate (SFR)
- SFR variation with time

19

## Measuring Star Formation (SF)

Galaxy spectra in the presence of young stars

The IMF

Observable consequences of SF

UV emission

Recombination lines

Free-Free emission

Dust emission

Wrinkles -- Obscured vs UnObscured, IMF variations

SF rates

Typical galaxies

ULIRGS

Dwarfs

20

# Why is measuring SFR important?

Converting gas into stars is a major evolutionary pathway

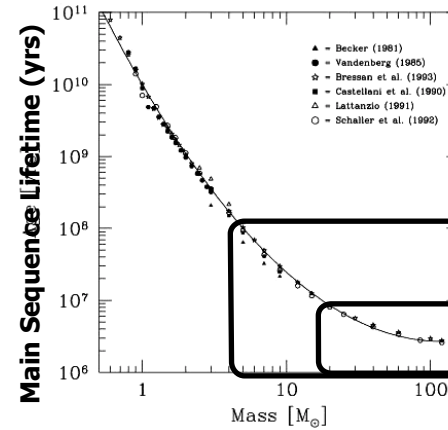
SFR affects SN feedback, production of metals, state of the ISM, galaxy luminosity and color...basically everything!

Should evolve with redshift

Need many indicators that work in different redshift regimes, and that can be checked against each other

21

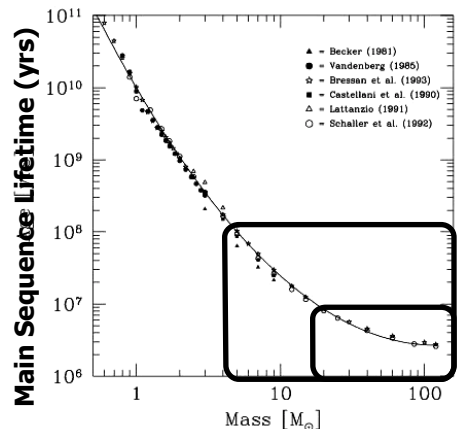
# Measuring the “instantaneous” SFR



Define “instantaneous” to be <10-100 Myr

22 <http://www.bo.astro.it/~eps/buz10201/ajf03.jpg>

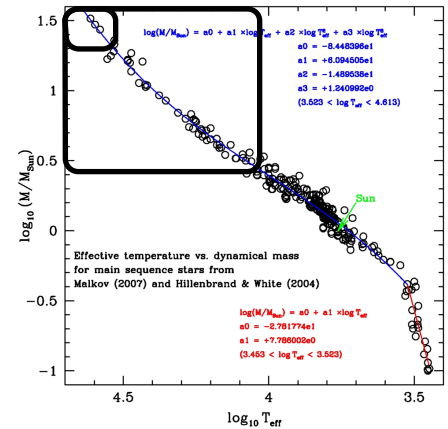
# Measuring the “instantaneous” SFR



Find tracers of  $>4-20 M_{\odot}$  (B & O) stars

23 <http://www.bo.astro.it/~eps/buz10201/ajf03.jpg>

# Measuring the “instantaneous” SFR



10-100Myr  $\rightarrow$  4-20  $M_{\odot}$   $\rightarrow$   $T_{\text{eff}} > 11,000-35,000\text{K}$

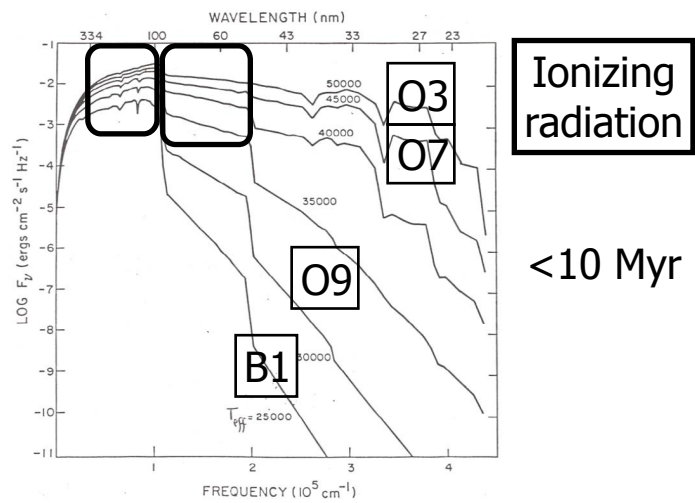
24

<http://www.pas.rochester.edu/~emamajek/codiplots.html>

## Signatures of >10,000-35,000K stars:

near- &  
far-UV  
flux

<100Myr



Ionizing  
radiation

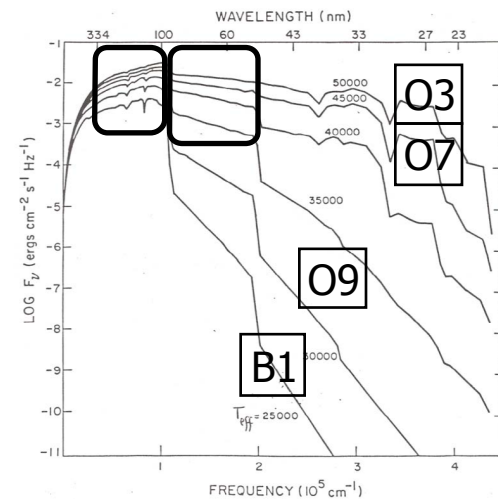
<10 Myr

25

## Current SFR Tracers:

near- &  
far-UV  
flux

<100Myr



Ionizing  
radiation

<10 Myr

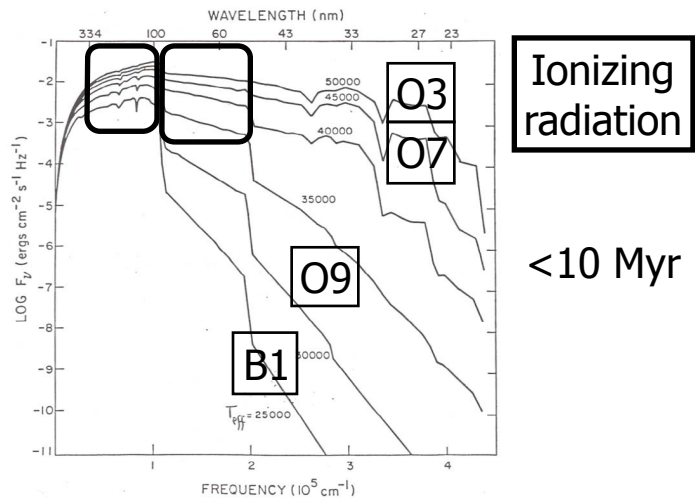
All amount to looking for UV flux or signs of ionized gas

26

## Current SFR Tracers:

near- &  
far-UV  
flux

<100Myr



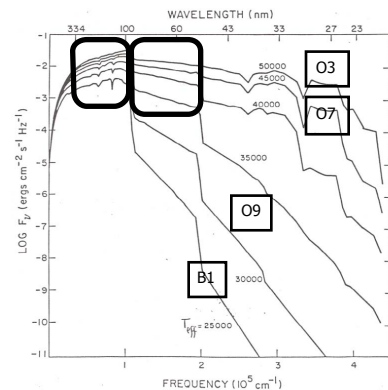
Ionizing  
radiation

<10 Myr

**But!!!** Must translate measurements of flux to quantitative SFR ( $M_{\odot}/\text{yr}$ )

27

**Total** UV & Ionizing Flux depends on exact numbers of very hot stars



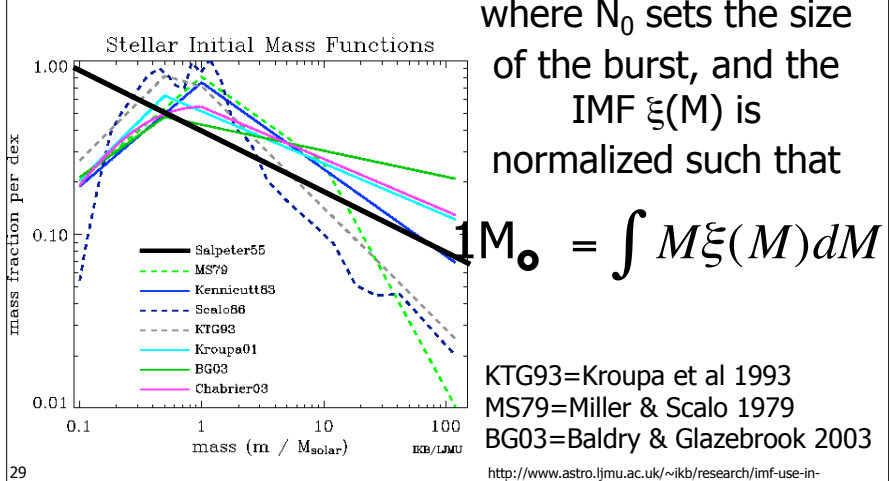
Converting to SFR ( $M_{\odot}/\text{yr}$ ) requires **extrapolating** to the total stellar mass associated with the detected O & B stars

Both depend sensitively on the "Initial Mass Function"

28

## The Initial Mass Function (IMF):

$$\# \text{stars with } M \rightarrow M + dM = N_0 \xi(M) dM$$



29

where  $N_0$  sets the size of the burst, and the IMF  $\xi(M)$  is normalized such that

$$1 M_{\odot} = \int M \xi(M) dM$$

KTG93=Kroupa et al 1993  
MS79=Miller & Scalo 1979  
BG03=Baldry & Glazebrook 2003

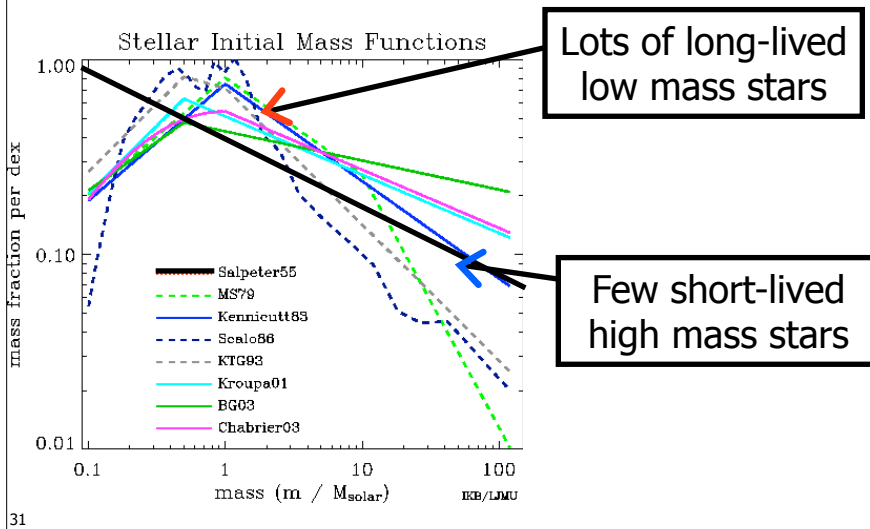
IMF is frequently approximated as a power law

$$\xi(M) \propto M^{-(1+x)}$$

If  $x=1.35$ , you get the "Salpeter IMF"

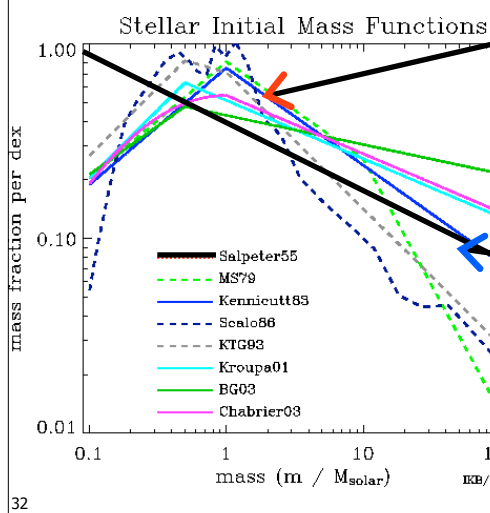
30

## The Initial Mass Function (IMF):



31

## The Initial Mass Function (IMF):



32

$$L_{MS} \propto M^{+3.5}$$

$$L\xi(M) \propto M^{+1.15}$$

## IMF variations for low mass stars

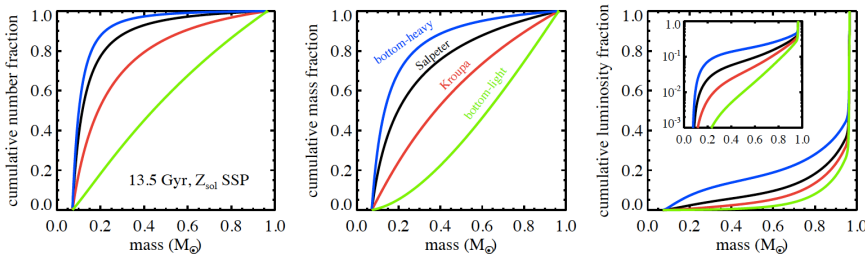
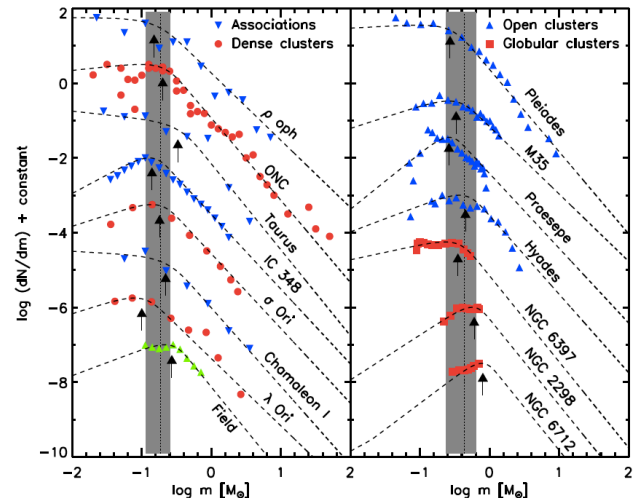


Figure 4:

Fractional contribution to the total number, mass, and bolometric luminosity as a function of stellar mass for a 13.5 Gyr solar metallicity model. Lines correspond to different IMFs: a bottom-heavy with logarithmic slope  $x = 3.0$  (blue line); Salpeter ( $x = 2.35$ ; black line); MW IMF (specifically a Kroupa IMF; red line); a bottom-light IMF (specifically of the form advocated by van Dokkum (2008); green line). The inset in the right panel shows the cumulative luminosity fraction in logarithmic units. Low mass stars dominate the total number and mass in stars, but contribute a tiny fraction of the luminosity of old stellar populations.

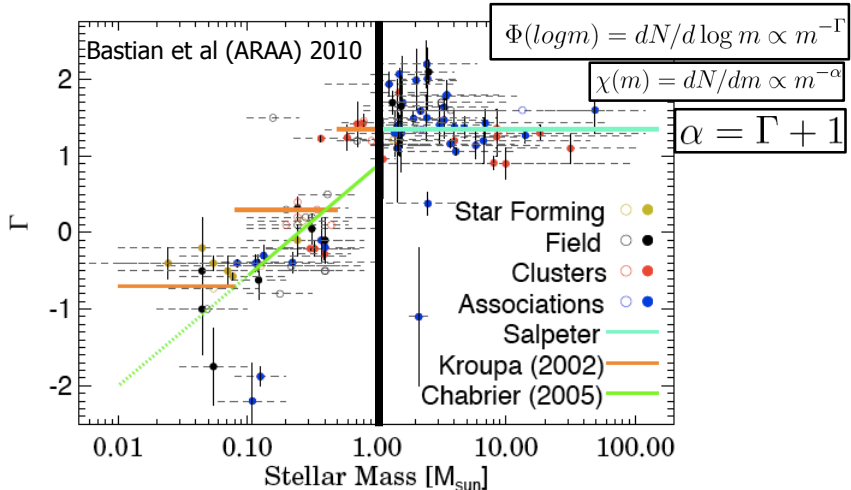
33 Conroy et al (ARA&A) 2013

## Derived typically from stellar clusters



34 Bastian et al (ARA&A) 2010

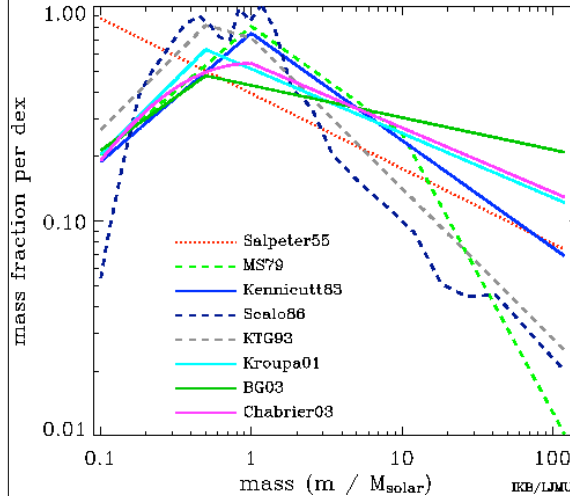
## Clear slope variations with mass



MW high-mass slope ( $> 1 M_{\odot}$ ) relatively constant

35

## Stellar Initial Mass Functions

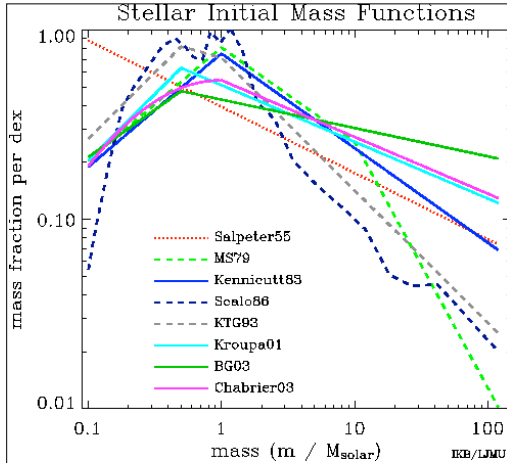


IMF propagates into nearly every aspect of extragalactic astronomy

- The Kennicutt, Kroupa01, BG03 and Chabrier IMFs are the best fit for reasonable mass-to-light ratios and galaxy colors (solid lines). The BG03 analysis favoured a slope shallower than Salpeter at the high-mass end based on constraints from local luminosity densities and cosmic star-formation history; IMFs with high-mass slopes steeper than Kennicutt's were ruled out as a universal IMF.
- The Salpeter IMF has too many low mass stars (dotted line). It was never measured down to 0.1 solar masses by Salpeter.
- The MS79, Scalo and KTG93 IMFs have too few high mass stars (dashed lines). They were based on galactic disk measurements which cannot be used to accurately infer the high-mass end because of the complicated SFH of the galaxy. Measured IMFs within star clusters generally give a shallower IMF close to the Salpeter value. Elmegreen 06 finds that galaxy-averaged IMFs are not in general steeper than this.

36

<http://www.astro.ljmu.ac.uk/~ikb/research/imf-use-in-cosmolog>



The high-mass IMF slope has particularly large effects

- Metal production
- SN rates
- SN feedback
- Ionizing flux

- The Kennicutt, Kroupa01, BG03 and Chabrier IMFs are the best fit for reasonable mass-to-light ratios and galaxy colors (solid lines). The BG03 analysis favoured a slope shallower than Salpeter at the high-mass end and based on constraints from local luminosity densities and cosmic star formation history; IMFs with high-mass slopes steeper than Kennicutt's were ruled out as a universal IMF.
- The Salpeter IMF has too many low mass stars (dotted line). It was never measured down to 0.1 solar masses by Salpeter.
- The MS79, Scalo and KT93 IMFs have too few high mass stars (dashed lines). They were based on galactic disk measurements which cannot be used to accurately infer the high-mass end because of the complicated SFH of the galaxy. Measured IMFs within star clusters generally give a shallower IMF close to the Salpeter value. Elmegreen 06 finds that galaxy-averaged IMFs are not in general steeper than this.

37

<http://www.astro.ljmu.ac.uk/~ikb/research/imf-use-in-cosmolo>

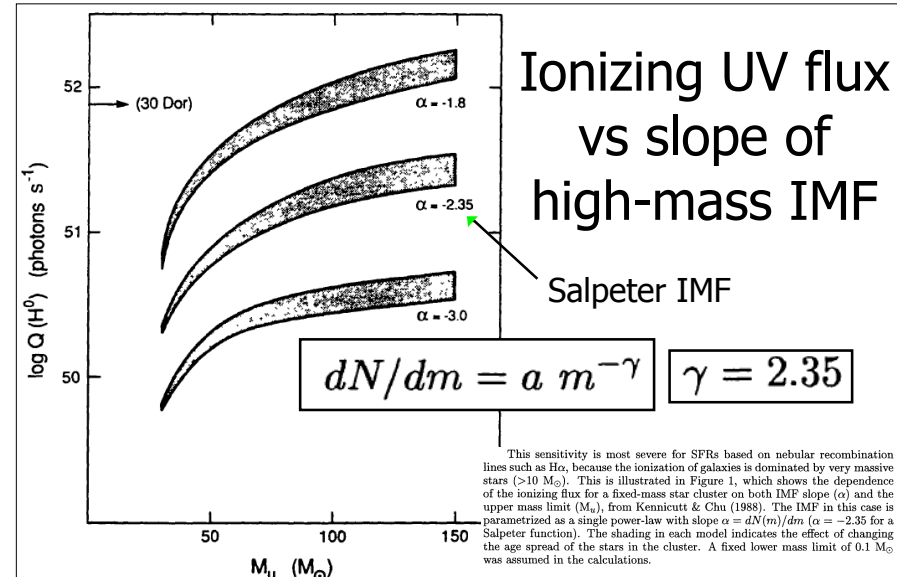


Figure 1. Initial ionizing luminosity for a star cluster with fixed mass (luminosity  $M_V = -9$  at age 100 Myr), as functions of the IMF slope  $\alpha$  and upper mass limit  $M_u$ , from Kennicutt & Chu (1988).

This sensitivity is most severe for SFRs based on nebular recombination lines such as H $\alpha$ , because the ionization of galaxies is dominated by very massive stars ( $>10 M_\odot$ ). This is illustrated in Figure 1, which shows the dependence of the ionizing flux for a fixed-mass star cluster on both IMF slope ( $\alpha$ ) and the upper mass limit ( $M_u$ ), from Kennicutt & Chu (1988). The IMF in this case is parameterized as a single power-law with slope  $\alpha = dN(m)/dm$  ( $\alpha = -2.35$  for a Salpeter function). The shading in each model indicates the effect of changing the age spread of the stars in the cluster. A fixed lower mass limit of  $0.1 M_\odot$  was assumed in the calculations.

## Back to calculating SFRs...

Convert tracers of  $>4-20 M_\odot$  (B & O) stars to quantitative values for the SFR

Use “stellar population synthesis models” w/ adopted IMF to calculate mapping from SFR to observables

- Usually assumes constant SFR for  $>100$  Myr

Use SFRs derived from older/reliable measurement to calibrate newer/less-reliable method

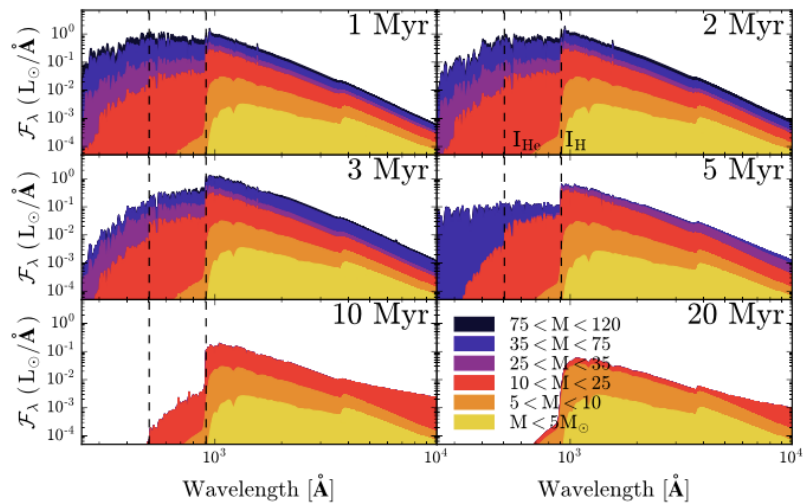
## Most direct constraint on ionizing flux

- Recombination lines of Hydrogen
  - Directly traces the numbers of ionizing photons
  - Effectively “counts” emission from O-stars
  - Ly $\alpha$  may have issues with being resonance line...
  - May not be photoionized by O-stars. Can have contributions from other sources of ionization (i.e., AGN, shocks)

40

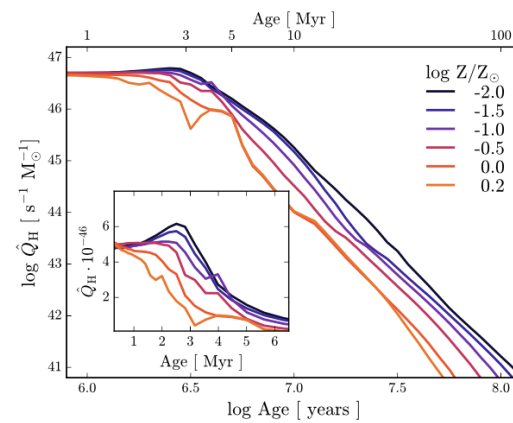
39

## Time scales & sources of ionizing flux



<sup>41</sup> Byler et al 2017

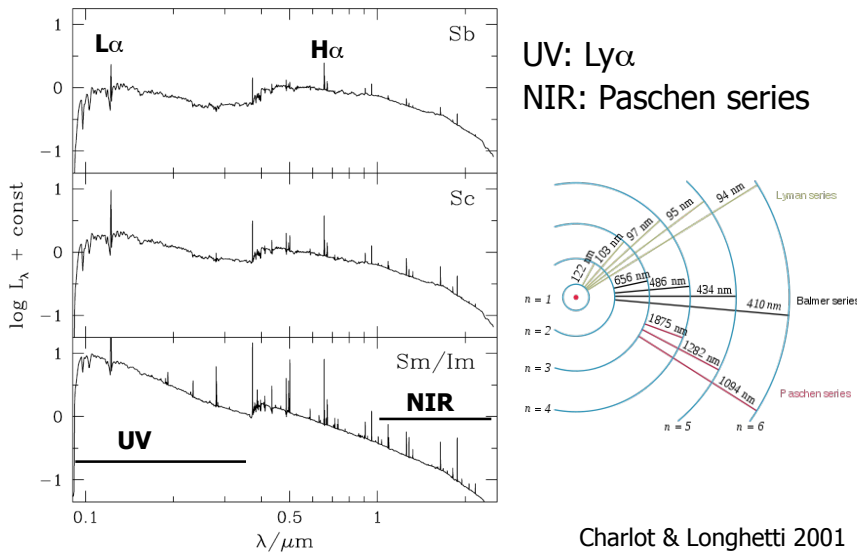
## Ionizing photon production down by x10 within ~7Myr



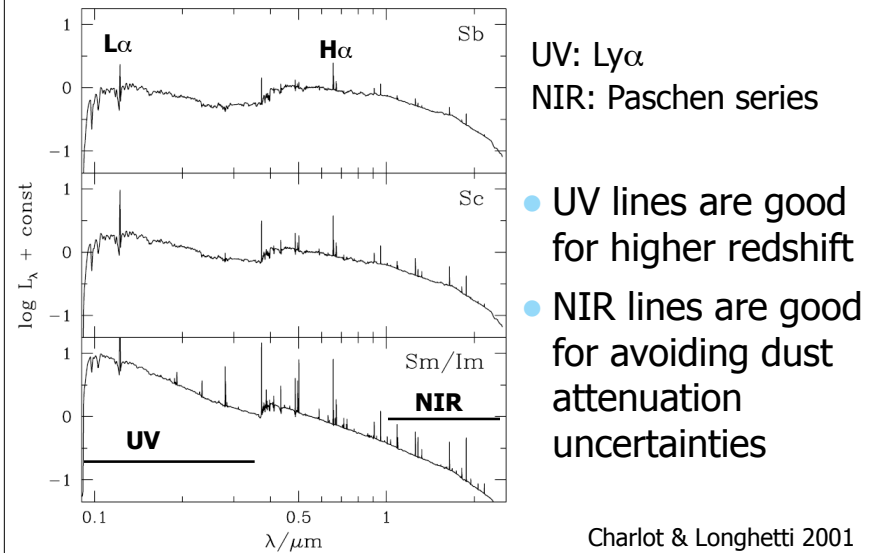
Recombination lines: very recent SF

<sup>42</sup> Byler et al 2017

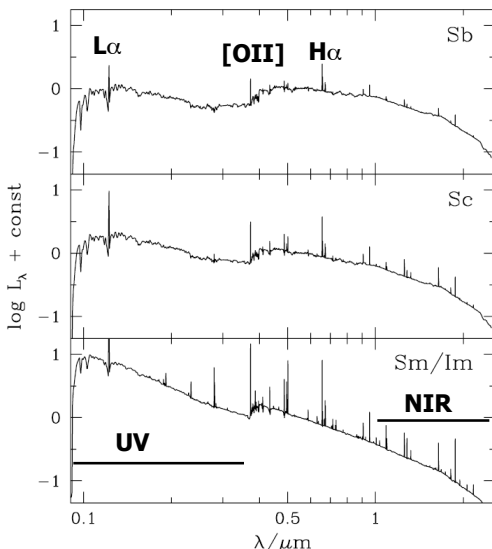
## Recombination lines appear in the UV, IR, and even radio



## Recombination lines appear in the UV, IR, and even radio

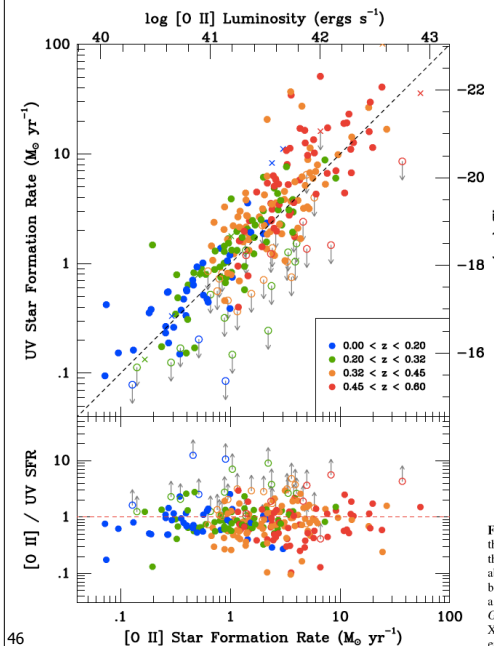


Forbidden lines are used as well, but:



- Less direct tracer of ionization
- Depends on metallicity, ionization parameter
- But, only lines accessible at some redshifts (e.g., [OII] doublet at 3727A appears between Ly $\alpha$  and H $\alpha$ )

Charlot & Longhetti 2001



Ciardullo et al 2013

Example of calibrating [OII] forbidden line as SFR indicator

For references: Wavelengths of emission lines

Table I. Computed lines: Hydrogen recombination lines (upper pannel), E lithium and metal lines (lower pannel)

Ly $\alpha$ 1216	Ly $\beta$ 1025	Ly $\gamma$ 972	Ly $\delta$ 949	Ly 937	Ly 930
Ly 926	Ly 922	H $\alpha$ 6563	H $\beta$ 4861	H $\gamma$ 4340	H $\delta$ 4102
H 3970	H 3889	H 3835	H 3798	Pa $\alpha$ 18752	Pa $\beta$ 12819
Pa $\gamma$ 10939	Pa $\delta$ 10050	Pa 9546	Pa 9229	Pa 9015	Pa 8863
Br $\alpha$ 40515	Br $\beta$ 26254	Br $\gamma$ 21657	Br $\delta$ 19447	Br 18175	Br 17363
Br 16808	Br 16408	Pf $\alpha$ 74585	Pf $\beta$ 46529	Pf $\gamma$ 37398	Pf $\delta$ 32964
Pf 30386	Pf 28724	Pf 27577	Pf 26746	Hu $\alpha$ 123690	Hu $\beta$ 75011
Hu $\gamma$ 59071	Hu $\delta$ 51277	Hu 46716	Hu 43756	Hu 41700	Hu 40201
HeII 1640	HeII 1217	HeII 1085	HeII 4686	HeII 3203	HeII 2733
HeII 2511	HeI 4471	HeI 5876	HeI 6678	HeI 10830	HeI 3889
HeI 7065	[CI] 9850	[CI] 8727	[CI] 4621	[CI] 609 $\mu$ m	[CI] 369 $\mu$ m
[CII] 157.7 $\mu$ m	CII 2326	CIII 1908	[NI] 5199	[NI] 3466	[NI] 10400
[NII] 6584	[NII] 6548	[NII] 5755	[NII] 122 $\mu$ m	[NII] 205 $\mu$ m	[NII] 2141
[NIII] 57 $\mu$ m	[OI] 6300	[OI] 6363	[OI] 5577	[OI] 63 $\mu$ m	[OI] 145 $\mu$ m
[OII] 3727	[OII] 7325	[OII] 2471	OIII 1663	[OIII] 5007	[OIII] 4959
[OIII] 4363	[OIII] 2321	[OIII] 88 $\mu$ m	[OIII] 52 $\mu$ m	[OIV] 26 $\mu$ m	[NeII] 13 $\mu$ m
[NeIII] 15.5 $\mu$ m	[NeIII] 36 $\mu$ m	[NeIII] 3869	[NeIII] 3967	[NeIII] 3343	[NeIII] 1815
[NeIV] 2424	[NeIV] 4720	MgII 2800	[SiII] 35 $\mu$ m	[SII] 10330	[SII] 6731
[SIII] 6717	[SIII] 4070	[SIII] 4078	[SIII] 19	[SIII] 33.5	[SIII] 9532
[SIII] 9069	[SIII] 6312	[SIII] 3722	[SIV] 10.4 $\mu$ m	[ArII] 69850	[ArIII] 7135
[ArIII] 7751	[ArIII] 5192	[ArIII] 3109	[ArIII] 3005	[ArIII] 22 $\mu$ m	[ArIII] 9 $\mu$ m

Second constraint on ionizing flux

- Free-free bremsstrahlung emission from electrons
  - Easy to measure from the ground (1.4 GHz, 4.3 GHz widely used)
  - Unaffected by dust

## VLA map at 20cm

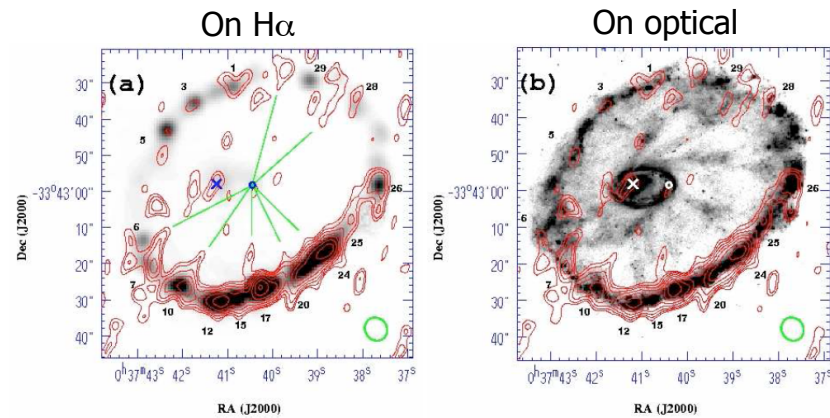


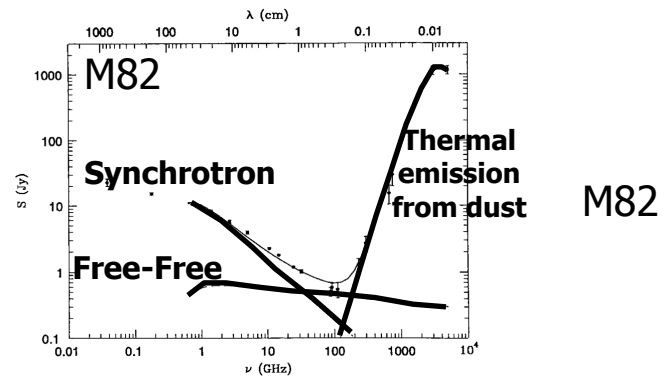
FIG. 1.— 20 cm RC intensity contours of the Cartwheel superimposed on (a) an H $\alpha$  image (gray scale), which has been smoothed to the resolution of the 20 cm B-band image, and (b) the HST B-band image. The lowest contour level corresponds to  $60 \mu\text{Jy beam}^{-1}$  ( $\approx 2\sigma$ ), and the subsequent contour levels increase by a factor of  $\sqrt{2}$ . The ellipse at the bottom-right corner indicates the RC beam size. In (a) note the excellent positional correspondence between radio peaks and H $\alpha$  complexes, which have been labeled by their H95 numbers. Straight lines are drawn connecting the filamentary structures or *spokes* to the geometrical center of the ring. Unlike the optical spokes (features connecting the inner ring to the outer ring in (b)), the RC spokes are straight and short. The position of the nucleus is marked by a cross.

49

Mayya et al 2005

## Free-Free emission caveat

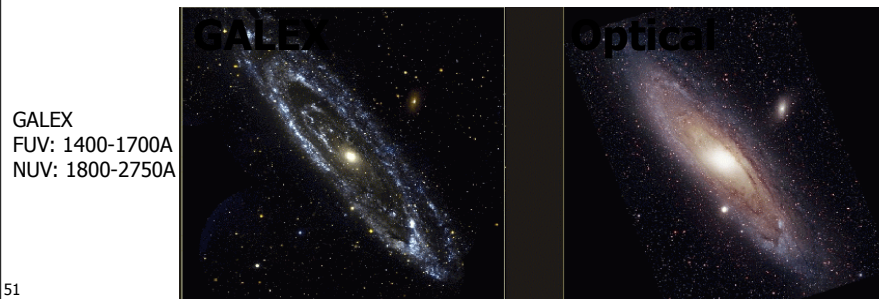
Contaminated by non-thermal emission (synchrotron), which also depends on SFR, but in an unpredictable way.



50

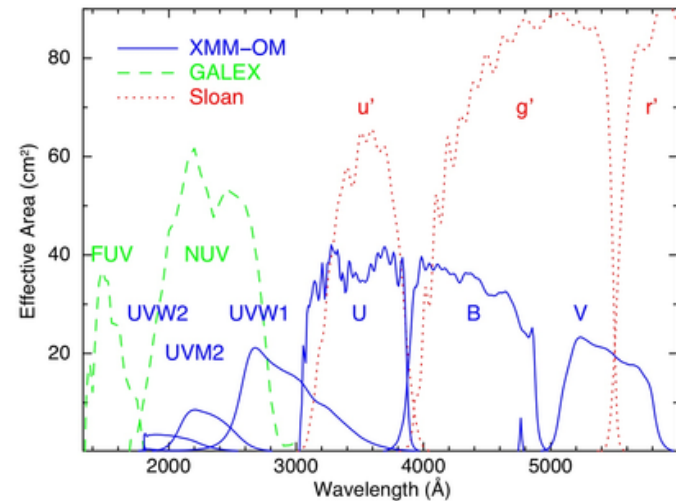
## Direct constraints on UV flux

- Measure the UV flux directly
  - Shorter wavelengths more sensitive to recent SF (higher mass stars), but requires space
  - Strongly affected by dust



51

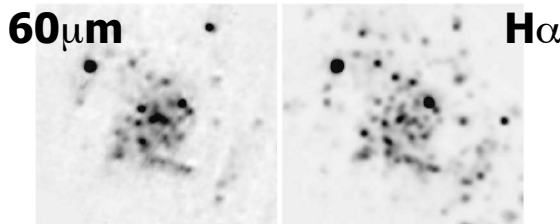
## Galex & Swift



52

## Indirect constraints on UV flux

- Measure mid- and far-IR (FIR) emission from dust to track reprocessed UV flux
  - depends on metallicity, dust optical depth
  - must avoid contamination from cold dust



Tuffs &  
Popescu 2005

FIGURE 3. Left: Distribution of the localised warm dust component at  $60\mu\text{m}$ ,  $F_{60}^{\text{b}}$ , in M 33 (Hippelein et al. [42]). This is the scaled difference map  $2(F_{60} - 0.165 \times F_{160})$ , with the factor 0.165 given by the average flux density ratio  $F_{60}/F_{170}$  in the interarm regions. Right:  $H\alpha$  map of M 33 convolved to a resolution of  $60''$ .

At fixed SFR, FIR emission varies with amount of dust, so  $24\mu\text{m}$  not perfect SFR indicator on its own

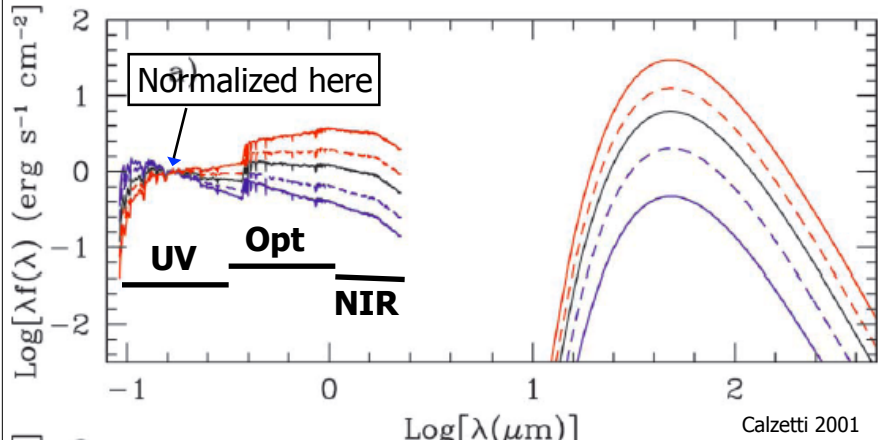
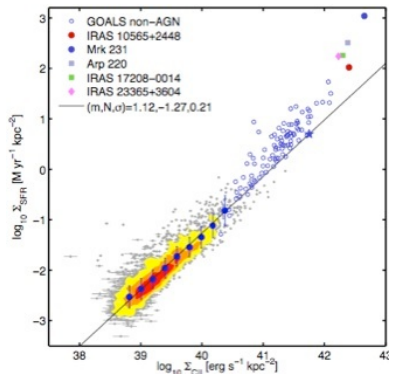


FIG. 11.—UV-to-IR SED of a 1 Gyr constant star formation population, attenuated by the starburst obscuration curve (eq. [8]), is shown for increasing amounts of dust:  $E(B-V)_{\mu\text{m}} = 0.05$  (blue solid line), 0.20 (blue dashed line), 0.40 (black), 0.55 (red dashed line), and 0.75 (red solid line). All SEDs are arbitrarily normalized to the flux density at  $0.17\mu\text{m}$ . The infrared SED is schematically represented by a single-temperature dust component with (a)  $T = 50\text{ K}$  and  $\epsilon = 2$  and (b)  $T = 40\text{ K}$  and  $\epsilon = 1.5$  to highlight differences in the long-wavelength regime.

## Indirect constraints on UV flux

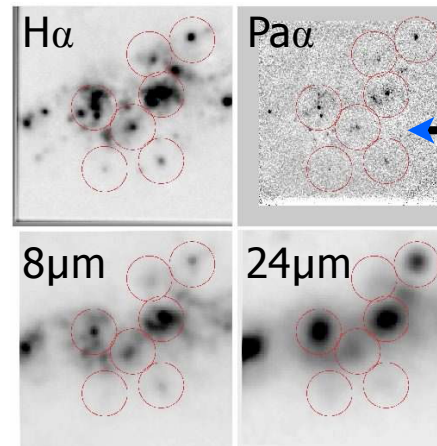
- Measure FIR [CII] cooling line
  - If cooling = heating, should constrain UV
  - Potential method w/ ALMA



**Calibrate w/  
KINGFISH  
Herschel survey  
of nearby  
galaxies**

Herrera-Camus  
et al

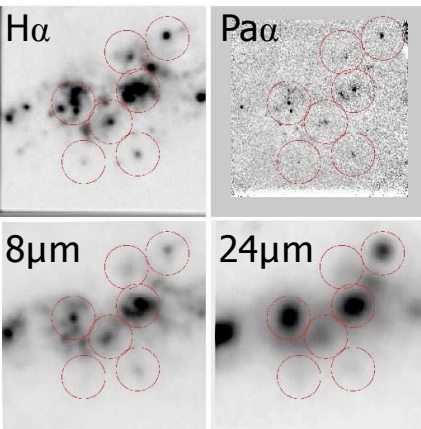
## Turning IR obs into Star Formation Rates



Assume Paα is  
“ground truth”  
(NIR, so little  
extinction)

56 Calzetti et al 2007

## Calibrating IR Star Formation Indicators



Verify relationship is linear, and compare to models

Note: 8micron does not look nearly as linear.

<sup>57</sup> Calzetti et al 2007

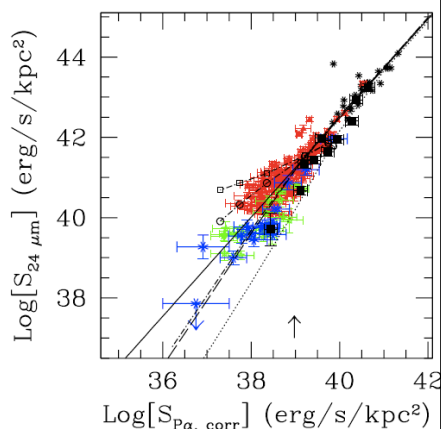


Fig. 9.—Luminosity surface density at 24  $\mu\text{m}$  as a function of the extinction-corrected Pa $\alpha$  LSD for the same datapoints as Figure 4 (after removal of the S2 2 nuclei, the foreground and background sources, and the NGC 2264 HII knot data), leaving 164 independent points to fit the linear calibration relations. The continuous line shows the best linear fit through the high-metallicity HII knots, from Figure 1. Models of infrared and ionized gas emission are superimposed on the data, for a variety of star formation histories, stellar initial mass functions, and metallicities (see Appendix). Models with solar metallicity ( $Z = Z_\odot$ ), IMF and stellar initial mass function, 100 Myr-old constant mass (SFR) ( $10^3 \text{ M}_\odot \text{ yr}^{-1}$ ), long dash line; instantaneous burst with variable mass ( $10^3 \text{ M}_\odot \text{ yr}^{-1}$ ) and coke-oven age, and constant age of 4 Myr (dot-dashed line); instantaneous burst with constant mass ( $10^3 \text{ M}_\odot \text{ kpc}^{-3}$ ) and variable age, and both variable mass ( $10^3 \text{ M}_\odot \text{ kpc}^{-3}$ ) and coke-oven age, and constant age of 4 Myr (dotted line); instantaneous burst with linear-star-forming rate and coke-oven age, and both variable mass ( $10^3 \text{ M}_\odot \text{ kpc}^{-3}$ ) and coke-oven age, and constant age of 4 Myr (dash-dot line); and a 1/10  $Z_\odot$  model of constant star formation over the past 100 Myr. The upward-pointing arrow marks the apparent luminosity where the transition between single-photon heating and thermal equilibrium occurs for the 24  $\mu\text{m}$  emission line.

## SFR's ( $M_\odot/\text{yr}$ ) from measured luminosities:

Kennicutt & Evans 2012

$$\log \dot{M}_*(M_\odot \text{ year}^{-1}) = \log L_x - \log C_x$$

Table 1 Star-formation-rate calibrations

Band	Age range (Myr) <sup>a</sup>	$L_x$ units	$\log C_x$ <sup>b</sup>	$\dot{M}_*/M_*(\text{K98})$ <sup>c</sup>	Reference(s)
FUV	0-10-100	ergs s <sup>-1</sup> ( $v L_\odot$ )	43.35	0.63	Hao et al. (2011), Murphy et al. (2011)
NUV	0-10-200	ergs s <sup>-1</sup> ( $v L_\odot$ )	43.17	0.64	Hao et al. (2011), Murphy et al. (2011)
H $\alpha$	0-3-10	ergs s <sup>-1</sup>	41.27	0.68	Hao et al. (2011), Murphy et al. (2011)
TIR	0-5-100 <sup>d</sup>	ergs s <sup>-1</sup> (3-1100 $\mu\text{m}$ )	43.41	0.86	Hao et al. (2011), Murphy et al. (2011)
24 $\mu\text{m}$	0-5-100 <sup>d</sup>	ergs s <sup>-1</sup> ( $v L_\odot$ )	42.69		Rieke et al. (2009)
70 $\mu\text{m}$	0-5-100 <sup>d</sup>	ergs s <sup>-1</sup> ( $v L_\odot$ )	43.23		Calzetti et al. (2010b)
1.4 GHz	0-100	ergs s <sup>-1</sup> Hz <sup>-1</sup>	28.20		Murphy et al. (2011)
2-10 keV	0-100	ergs s <sup>-1</sup>	39.77	0.86	Ranalli et al. (2003)

<sup>a</sup>Second number gives mean age of stellar population contributing to emission; third number gives age below which 90% of emission is contributed.

<sup>b</sup>Conversion factor between SFR and the relevant luminosity, as defined by Equation 12 in Section 3.8.

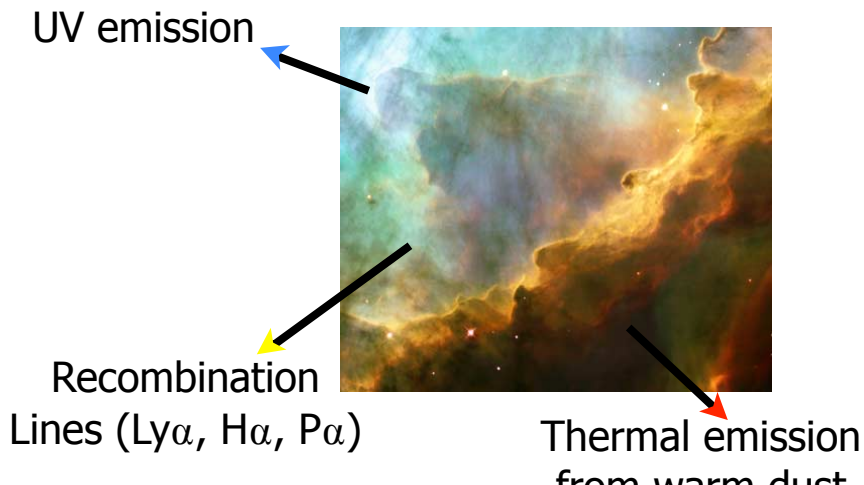
<sup>c</sup>Ratio of star-formation rate (SFR) derived using the new calibration to that derived using the relations in Kennicutt (1998a). The lower SFRs now mainly result from the different initial mass function and from updated stellar population models.

<sup>d</sup>Numbers are sensitive to star-formation history; those given are for continuous star formation over 0-100 Myr. For more quiescent regions (e.g., disks of normal galaxies), the maximum age will be considerably longer.

Abbreviations: FUV, far ultraviolet; NUV, near ultraviolet; TIR, total infrared.

Typically calculated from models of stellar populations where the SFR is constant over the lifetime of O/B stars ( $\sim 10^8$  yrs). Sensitive to the assumed IMF and upper mass cutoff.

## Obscured vs Unobscured SF



## Obscured vs Unobscured SF

Total SF requires “counting” all photons from O-stars.



Need to sum up SF inferred from both obscured and unobscured UV photons.

$$L_{\text{UV}}(\text{corr}) = L_{\text{UV}}(\text{observed}) + \eta L_{\text{IR}}$$

# Summary of corrections:

**Table 2** Multiwavelength dust corrections for normal galaxies

Composite tracer	Reference
$L(\text{FUV})_{\text{corr}} = L(\text{FUV})_{\text{obs}} + 0.46 L(\text{TIR})$	Hao et al. (2011)
$L(\text{FUV})_{\text{corr}} = L(\text{FUV})_{\text{obs}} + 3.89 L(25 \mu\text{m})$	Hao et al. (2011)
$L(\text{FUV})_{\text{corr}} = L(\text{FUV})_{\text{obs}} + 7.2 \times 10^{14} L(1.4 \text{ GHz})^a$	Hao et al. (2011)
$L(\text{NUV})_{\text{corr}} = L(\text{NUV})_{\text{obs}} + 0.27 L(\text{TIR})$	Hao et al. (2011)
$L(\text{NUV})_{\text{corr}} = L(\text{NUV})_{\text{obs}} + 2.26 L(25 \mu\text{m})$	Hao et al. (2011)
$L(\text{NUV})_{\text{corr}} = L(\text{NUV})_{\text{obs}} + 4.2 \times 10^{14} L(1.4 \text{ GHz})^a$	Hao et al. (2011)
$L(\text{H}\alpha)_{\text{corr}} = L(\text{H}\alpha)_{\text{obs}} + 0.0024 L(\text{TIR})$	Kennicutt et al. (2009)
$L(\text{H}\alpha)_{\text{corr}} = L(\text{H}\alpha)_{\text{obs}} + 0.020 L(25 \mu\text{m})$	Kennicutt et al. (2009)
$L(\text{H}\alpha)_{\text{corr}} = L(\text{H}\alpha)_{\text{obs}} + 0.011 L(8 \mu\text{m})$	Kennicutt et al. (2009)
$L(\text{H}\alpha)_{\text{corr}} = L(\text{H}\alpha)_{\text{obs}} + 0.39 \times 10^{13} L(1.4 \text{ GHz})^a$	Kennicutt et al. (2009)

<sup>a</sup>Radio luminosity in units of ergs s<sup>-1</sup> Hz<sup>-1</sup>.

Abbreviations: FUV, far ultraviolet; NUV, near ultraviolet; TIR, total infrared.

See updated relations in Boquien et al 2016

Kennicutt & Evans 2012

61

# Summary of corrections:

**Table 1.** SFR estimators.

Monochromatic				
Band	$\log C_{\text{band}}$	k	Method	Reference
FUV	-36.355	1.0000	Theoretical <sup>a</sup>	1
$\text{H}\alpha$	-34.270	1.0000	Theoretical <sup>a</sup>	1
24 $\mu\text{m}$	-29.134	0.8104	$\text{H}\alpha^b$	2
70 $\mu\text{m}$	-29.274	0.8117	$\text{H}\alpha^b$	3
100 $\mu\text{m}$	-37.370	1.0384	$\text{H}\alpha^b$	3

Hybrid				
Band	$\log C_{\text{band1}}$	$k_{\text{band1-band2}}$	Method	Reference
$\text{H}\alpha+24 \mu\text{m}$	-34.270	0.031	$\text{H}\alpha^b$	2
FUV+24 $\mu\text{m}$	-36.355	6.175	$\text{H}\alpha+24 \mu\text{m}$	4

References. (1) Murphy et al. (2011), (2) Calzetti et al. (2007), (3) Li et al. (2013), (4) Leroy et al. (2008)

Notes. Monochromatic:  $\log \text{ESFR} = \log C_{\text{band}} + k \times \log S_{\text{band}}$ ; Hybrid:  $\log \text{ESFR} = \log C_{\text{band1}} + \log [S_{\text{band1}} + k_{\text{band1-band2}} \times S_{\text{band2}}]$ , with  $\text{ESFR}$  in  $M_{\odot} \text{ yr}^{-1} \text{ kpc}^{-2}$ ,  $S$  defined as  $S_{\nu}$  in  $\text{W kpc}^{-2}$ , and  $C$  in  $M_{\odot} \text{ yr}^{-1} \text{ W}^{-1}$ .

Empirical estimators have been calibrated on individual star-forming regions on typical scales of the order of ~200–500 pc.

<sup>a</sup> Based on Starburst99 (Leitherer et al. 1999). <sup>b</sup> Extinction corrected, calibrated against near-infrared hydrogen recombinations lines (e.g., Paα or Brγ).

Boquien et al 2015

## What fraction of star formation is obscured?

Can characterize with  $\text{IRX} = \log \left( \frac{L(\text{TIR})}{L(\text{FUV})_{\text{obs}}} \right)$

Where the total IR luminosity is defined from Spitzer (SIRTF) fluxes. A simple combination of SIRTF Multiband Imaging Photometer fluxes recovers the total 3–1100  $\mu\text{m}$  flux (TIR) for the full range of normal galaxy infrared SED shapes,

$$L_{\text{TIR}} = \zeta_1 \nu L_{\nu}(24 \mu\text{m}) + \zeta_2 \nu L_{\nu}(70 \mu\text{m}) + \zeta_3 \nu L_{\nu}(160 \mu\text{m}),$$

where  $[\zeta_1, \zeta_2, \zeta_3] = [1.559, 0.7686, 1.347]$  for  $z = 0$ . (4)  
Def'n from Dale & Helou 2002

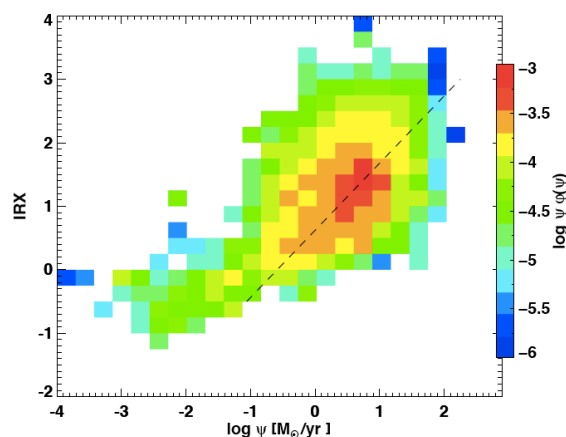
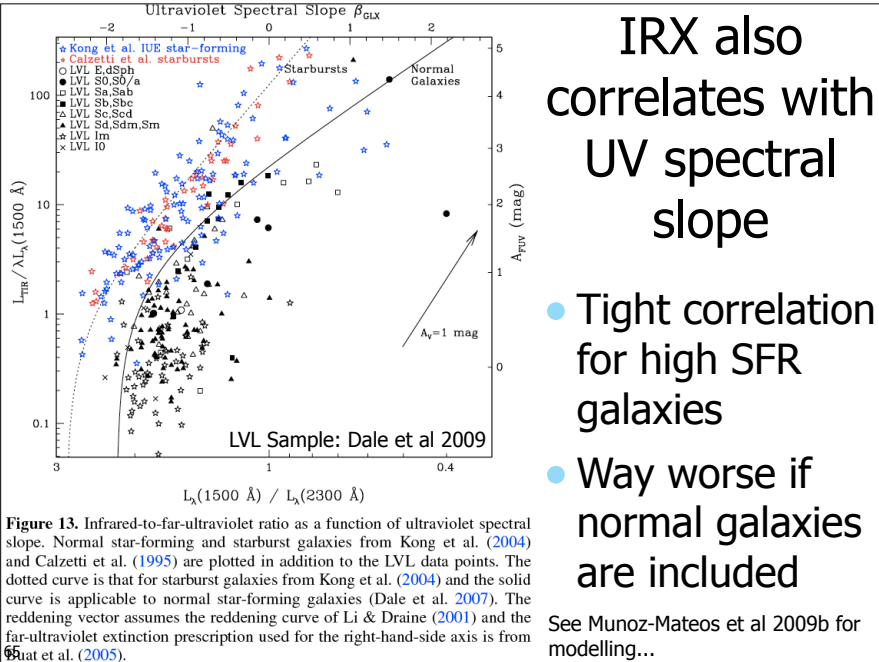


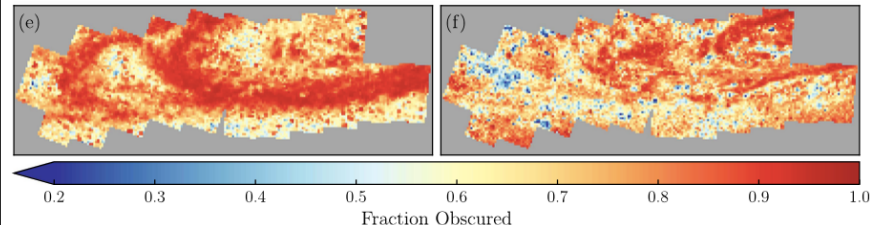
**Figure 10.** The star formation rate volume density function as a function of SFR (Fig. 5), further expanded in a second dimension (along the ordinate) to show the breakdown with IRX. The 'z' axis represents  $\psi \Phi(\psi)$ . The dotted line shows the IRX-SFR relationship derived from the  $\text{LIR}$  vs.  $E(B-V)$  relationship given by Hopkins et al. (2001).  $E(B-V)$  was converted into  $A_{\text{FUV}}$  using the Cardelli (1989) extinction law with  $R_V = 3.1$ , which gives  $A_{\text{FUV}} = 8.0 E(B-V)$ . IRX and  $\psi$  were obtained from  $A_{\text{FUV}}$  and  $\text{LIR}$  as above.  
Bothwell et al 2011

IRX is correlated with SFR:  
More obscuration when SFR is high

63



Prescriptions for obscured star formation break down in detail



True obscured fraction from CMD analysis

Obscured fraction from FUV+24 $\mu$

66 Alexia Lewis (UW) et al 2016

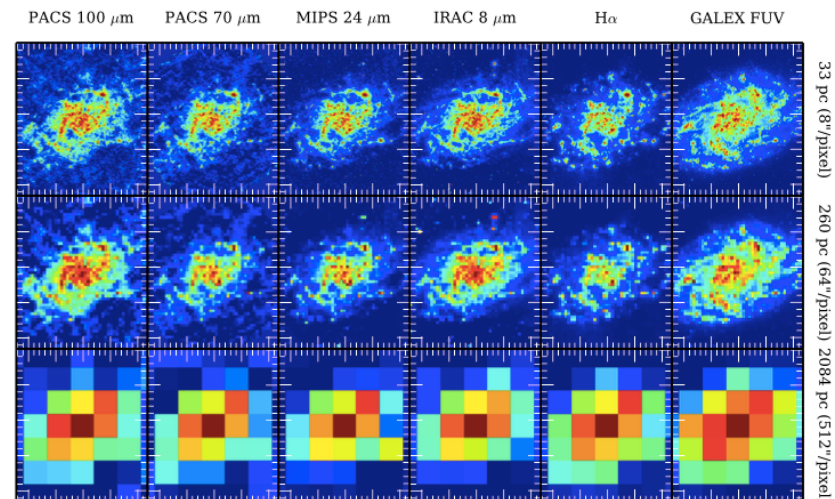
Major issue



The closer you get to the scale of individual SF regions, the more scaling laws will break down.

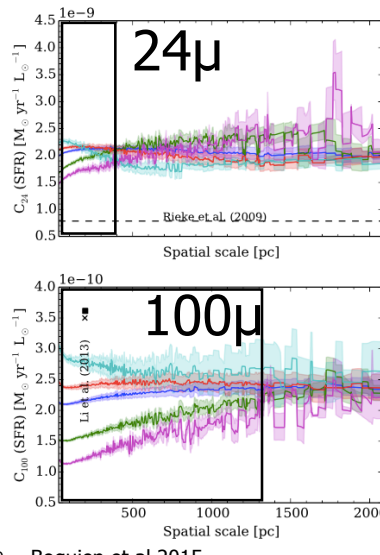
67

Example of SFRs vs scale (in M33)



68 Boquien et al 2015

## Example of SFRs vs scale (in M33)

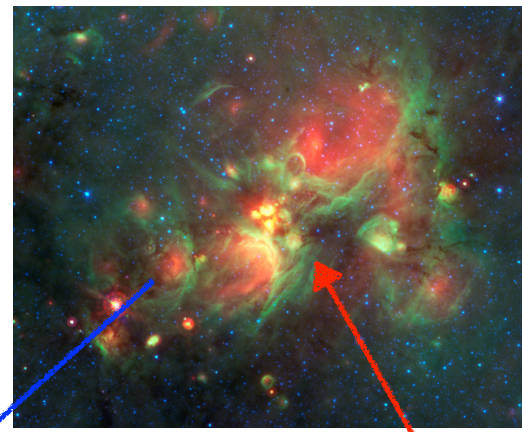


- Inferred SFR does not converge until 0.1-1.5kpc scales are reached
- Different behavior w/ different SFR tracers

**Fig. 6.** Scaling coefficients from the semi-analytic inferred Bieleke + SFR versus the physical scales for 24, 70, and 100  $\mu$ m, from the top level in all six bands. The blue line indicates the value of the scaling factor when taking into account pixels detected at  $\pm 1\sigma$  level in all six bands. The red (respectively green) line indicates the scaling factor when considering only pixels with a 2xSFR higher (resp. lower) than the median SFR at a given resolution. The cyan and magenta lines represent regions in the top and bottom 15% in terms of SFR. The black crosses indicate the scaling factor determined by Bieleke et al. (2009) (top), Li et al. (2013) (middle), and Li et al. (2010) (bottom). The grey crosses indicate the scaling factor determined by Bieleke et al. (2009) (red), Calentini et al. (2010) (green), Li et al. (2013) (blue), and Li et al. (2010) (black). The squares indicate mean values over several galaxies. The empty squares denote that no background subtraction was performed.

## Why do things break down?

Not all dust emission heated by SF

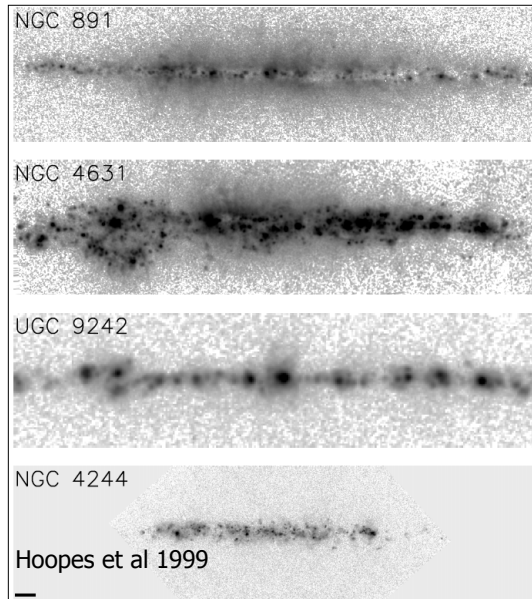


SFR not constant

UV emission escapes

Not all SF is in form of massive stars

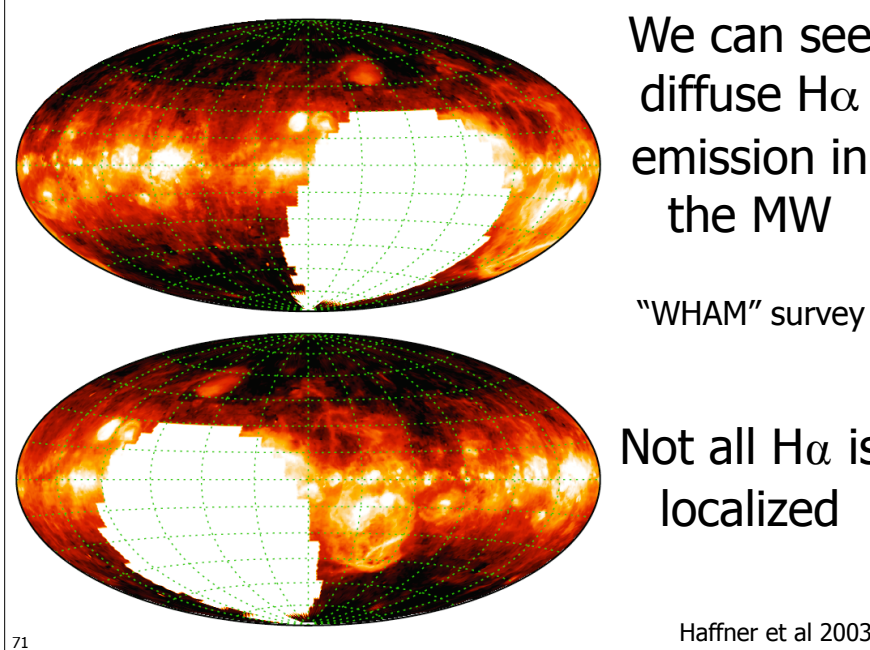
70



The diffuse component is vertically extended ("eDIG")

Large eDIG components are associated with galaxies with high star formation rates ("leakage" from HII regions?)

**Fig. 6.**—Comparison of the DIG layers in the galaxies in our sample. The images have been rotated so the disk is horizontal; see Figs. 1–5 for the correct orientation. The images all have the same spatial scale, shown by the 1 kpc bar in the bottom panel. They are all displayed with the same logarithmic stretch, from  $-2$  to  $1000 \text{ pc cm}^{-6}$ .



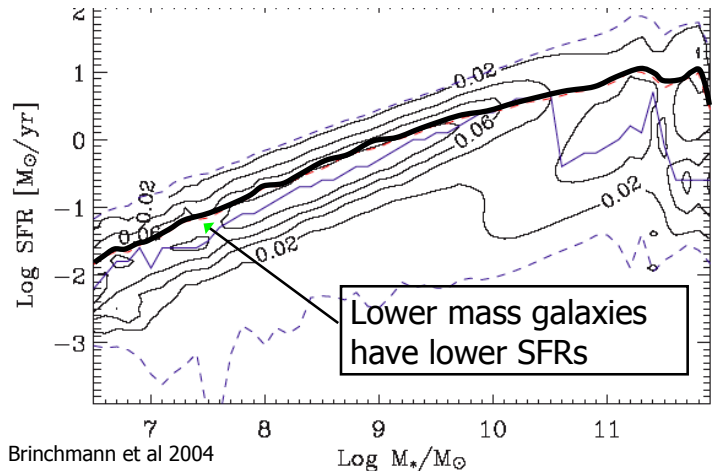
71

# Global Measures of Star Formation

- Star formation rates (SFR)
- Specific star formation rates (sSFR)
- Star Formation intensity ( $\Sigma_{\text{SFR}}$ )
- Star Formation efficiency

73

## 1. SFR: Increases with Stellar Mass



But, bigger things are  
bigger, so not profound...  
(calculated within SDSS fibers)

Brinchmann et al 2004

## 1. Total Star Formation Rates

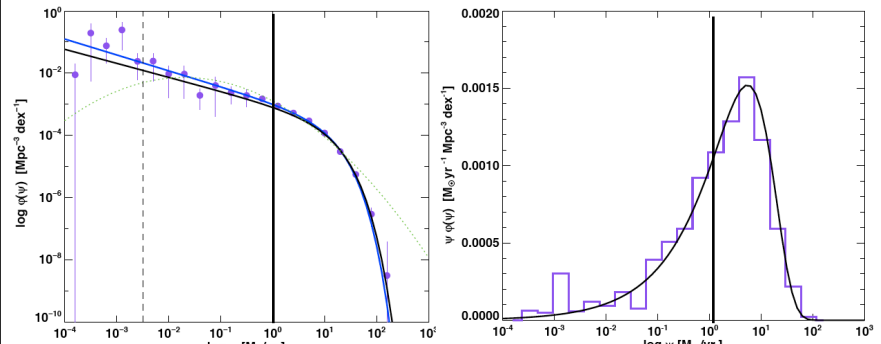


**Figure 4.** The star formation rate distribution function for the resultant combined sample, as described in §3.3. The black line is a least squares Schechter function fit to these points, the blue line is the maximum likelihood Schechter function fit. The vertical dashed line is drawn at  $\log \psi = -2.5 M_{\odot} \text{ yr}^{-1}$ , the level at which incompleteness becomes significant. The green log-normal function indicates the SFR function given by Martin et al. (2005). Errors ( $1\sigma$ ) were calculated using Monte Carlo bootstrapping.

Bothwell et al 2011

Most galaxies have low SFRs ( $< 1 M_{\odot}/\text{yr}$ ), but integrated SFR dominated by galaxies with  $\sim 10 M_{\odot}/\text{yr}$

74

## Fraction of total SFR density

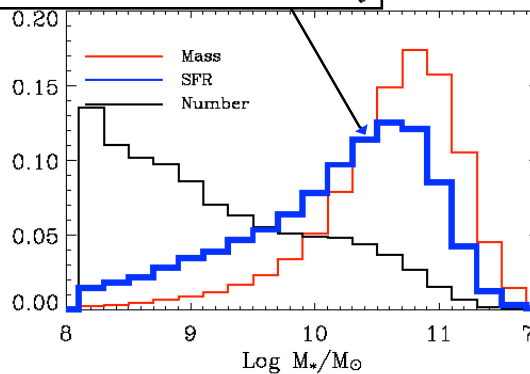


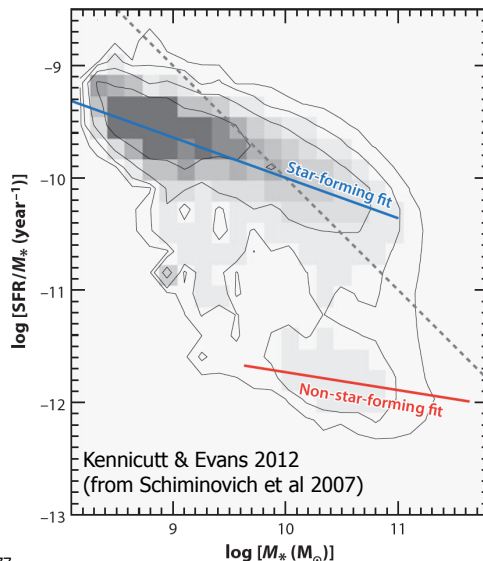
**Figure 20.** The contribution to the total number, mass and star formation density as a function of various galaxy parameters. The SF density is shown in blue, the mass density in red and the number density in black. *Top left:* The contribution to the different densities as a function of the concentration of the galaxies. *Top right:* The same, but as a function of the half-light radii of the galaxies. *Lower left:* The density contributions as a function of log stellar mass and *Lower right:* The contributions as a function of log of the stellar surface density in  $M_{\odot}/\text{kpc}^3$ .

Brinchmann et al 2004

Massive galaxies dominate the current production of stars, since they own most of the baryons

76

## 2. Specific SFR = SFR / stellar mass

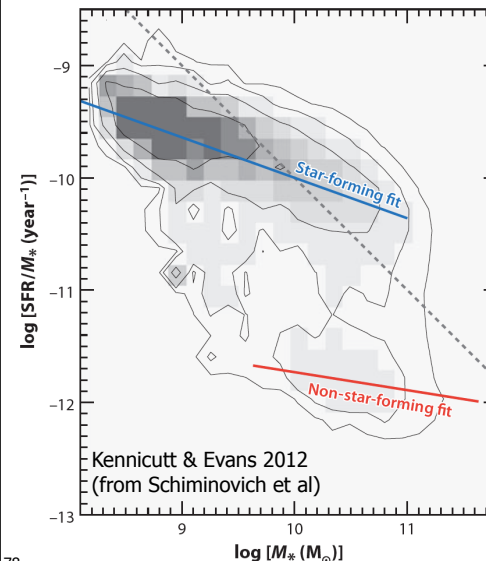


Relative importance of current to past SF

Units of inverse time  
(i.e., How long would it take to make the current stellar mass, at the current SFR)

77

## 2. sSFR shows two sequences



- “Red” and “Blue”
- Blue SF sequence
- “Green Valley”
- Red SF sequence

78

## 2. Related def'n of sSFR

Scalo Birthrate Parameter:  
Ratio of Current to Past SFR

$$b = \text{SFR}_{\text{now}} / \langle \text{SFR} \rangle$$

$b < 1$ : SFR greater in the past

$b = 1$ : SFR  $\sim$  constant

$b > 1$ : SFR higher today than in past

$b > 2-3$ : Classified as Starburst

Note:  $b$  alone does not distinguish between a steady increase in SF to the present day, or an episodic burst

## Measuring the Birthrate Parameter

$$b = \text{SFR}_{\text{now}} / \langle \text{SFR} \rangle$$

Use any SF indicator

Proportional to the total mass in stars  
( $\sim M_{\text{star}}/t_{\text{universe}}$ )

Will Correlate with lots of measures, like:

$$L_{\text{FIR}}/L_{\text{NIR}}$$

$$\text{SFR}/M_{\text{star}}$$

$$\text{H}\alpha \text{ Equivalent Width}$$

80

## 2. Specific SFR: Lower mass galaxies have systematically higher ssFR's

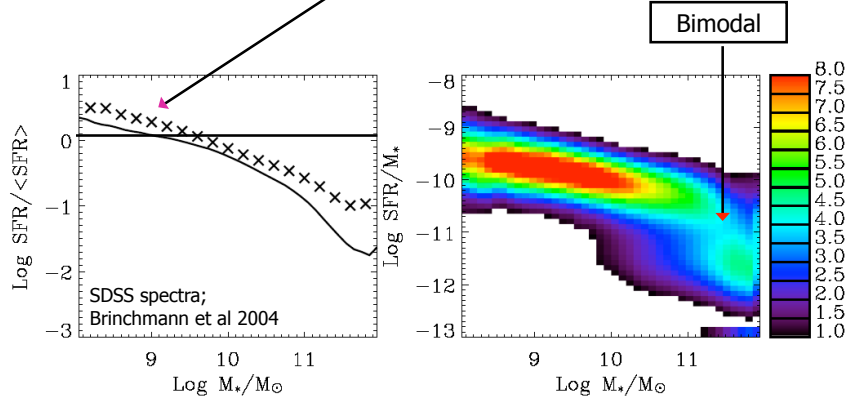


Figure 24. Similar to Figure 23 but this time showing  $b$  as a function of the stellar mass.

Figure 23. The specific SFR as a function of concentration. The left panel contrasts  $b^g$  with  $b^V$ . The continuous line in this plot shows the median of the unweighted  $b^g$  (right panel) and the crosses show  $b^V$  calculated from the data in Figure 20. The right hand panel shows the (log of the) observed likelihood distribution of  $r_{\text{SFR}}$  with respect to the concentration parameter,  $R_{90}/R_{50}$ , calculated as described in the text. The shading shows the conditional likelihood distribution (volume corrected) given a value for  $R_{90}/R_{50}$ . The contributions to the likelihood distributions below the plotted range have been put in the two lowest bins in  $r_{\text{SFR}}$ .

## 2. Specific SFR: Warning. H $\alpha$ can be stochastic in low mass galaxies

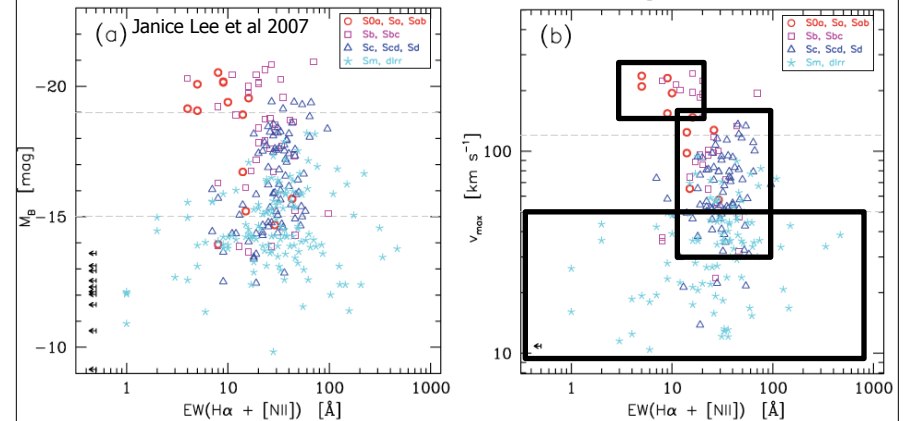
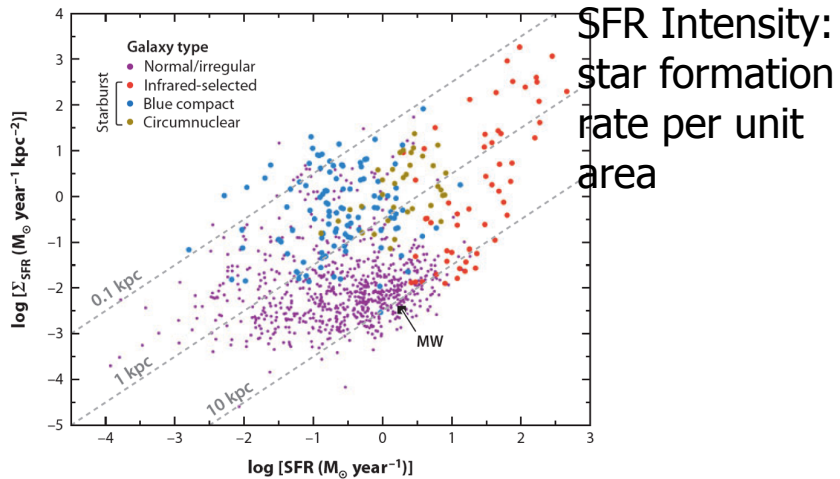


FIG. 1.—The Local Volume star-forming galaxy sequence in the (a)  $M_B$ -EW and the (b) rotational velocity-EW planes. Galaxies in the core sample of 11HUGS (i.e., those with  $T \geq 0$ ,  $D < 11$  Mpc, and  $|\delta| > 20^\circ$ ) are shown. Gray dashed lines are drawn at  $M_B = -19$  and  $V_{\text{max}} = 120$  km s $^{-1}$ , and  $M_B = -15$  and  $V_{\text{max}} = 50$  km s $^{-1}$  to indicate the two transition regions discussed in the text.

$H\alpha$  equivalent widths ( $\propto b$ ). FUV will be better

## 3. Star formation rate intensity ( $\Sigma_{\text{SFR}}$ )



Best proxy for local physical conditions, particularly in disks

## 4: SFR Efficiency: $\text{SFR} / M_{\text{gas}}$

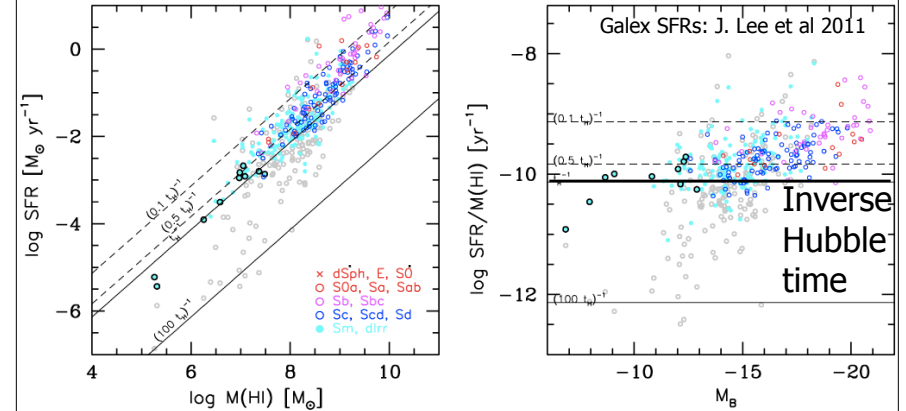
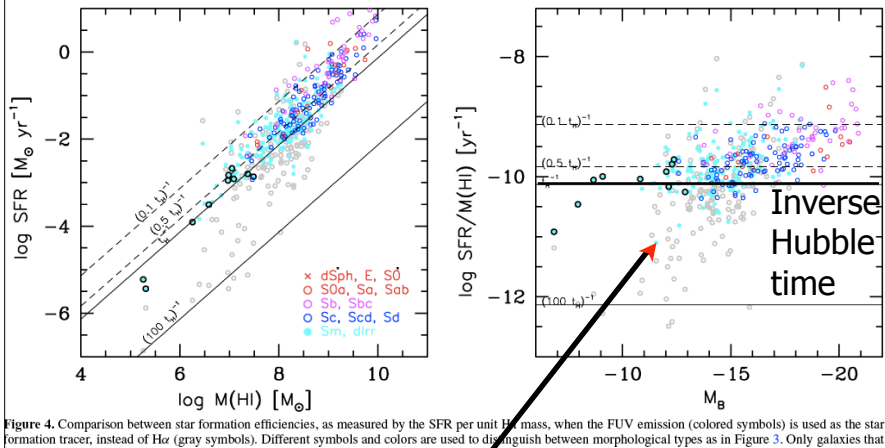


Figure 4. Comparison between star formation efficiencies, as measured by the SFR per unit H I mass, when the FUV emission (colored symbols) is used as the star formation tracer, instead of H $\alpha$  (gray symbols). Different symbols and colors are used to distinguish between morphological types as in Figure 3. Only galaxies that have both FUV and H $\alpha$  measurements are shown. Best-effort attenuation corrections are applied before computing the SFR as in Lee et al. (2009b).

Measure of timescale to consume all gas  
(Inverse = “gas consumption timescale”)

## 4. SFR Efficiency: $SFR / M_{\text{gas}}$



dIrrs would take close to a Hubble time to consume their gas  
Higher mass galaxies close to finished, if not resupplied

Galex SFRs: J. Lee et al 2011

85

## 4. SFR Efficiency: Milky Way

First Order:

$$M_{\text{stars,spiral}} = 10^{10} M_{\odot}$$

$$t_{\text{universe}} = 10^{10} \text{ yrs}$$

So, average:  
 $\langle SFR \rangle \sim 1 M_{\odot}/\text{yr}$

How long can this go on?

First Order:

$$M_{\text{gas}} = 10^9 M_{\odot}$$

$$\text{SFR} \sim 1 M_{\odot}/\text{yr}$$

So, average:  
 $t_{\text{gasconsumption}} \sim 10^9 \text{ yrs}$

So either we live in a special time where the MW is about to run out of gas, or there is on-going gas accretion to fuel continuing SF

86

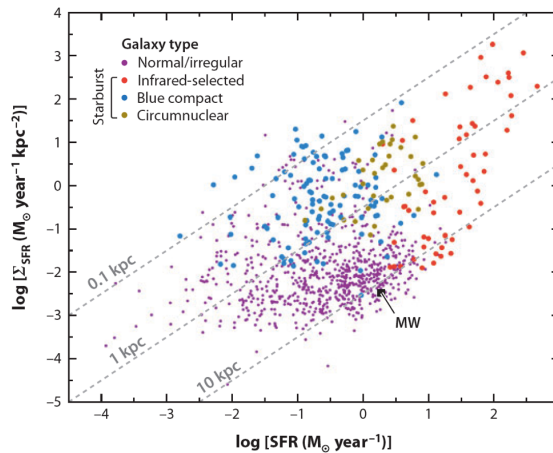
## Systems with High Star Formation

- High Star formation rates (SFR)
- High Star Formation intensity ( $\Sigma_{\text{SFR}}$ )
- High Specific star formation rates (sSFR)

1. Useful as probes of extreme conditions
2. Important phases in build-up of stars

87

## The High SFR End

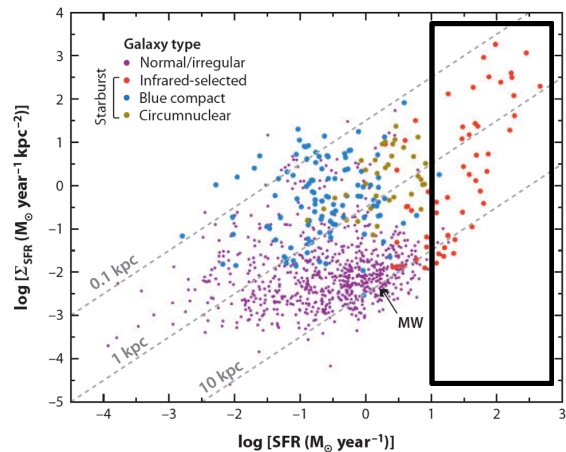


Possible Definitions of "High"

- High absolute SFRs
- High SFR intensities
- High SFRs compared to past average

88

## The High SFR End



Possible Definitions of "High"

- High absolute SFRs
- High SFR intensities
- High SFRs compared to past average

89

## "ULIRGS" (ultraluminous infrared galaxies) Highest SFRs (10-1000 M<sub>0</sub>/yr)

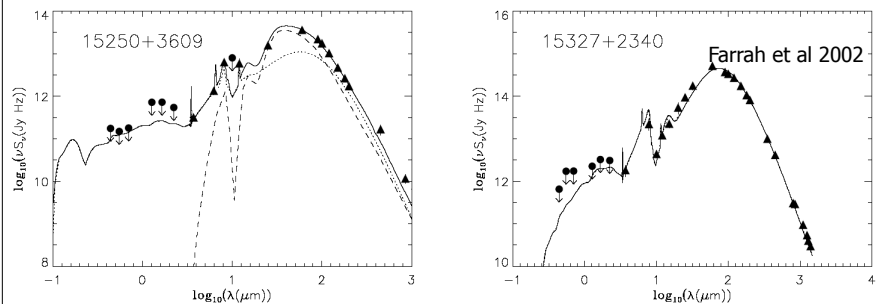
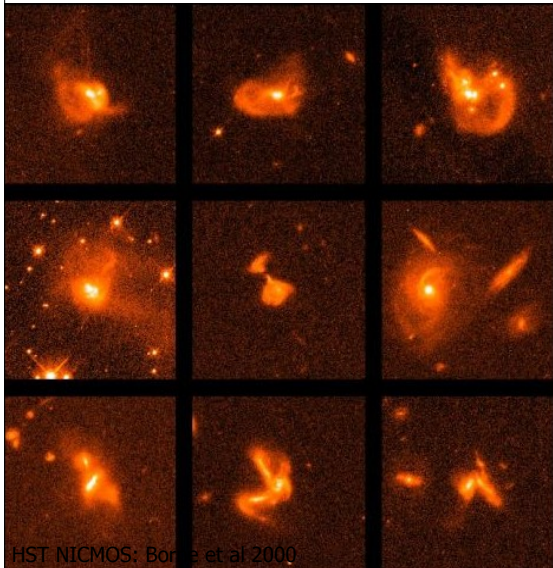


Figure 1. Best fit Spectral Energy Distributions for the 41 ULIRGs in our sample. In each case the solid line is the combined best-fit model, the dotted line is the Starburst component and the long dashed line is the AGN component.

- Majority of their enormous luminosity is reprocessed to FIR.
- Inconspicuous in optical because highly obscured.

90

## ULIRGS are almost universally massive major mergers



- Probably good local analogs of the formation of ellipticals at high redshift.
- These rare systems may actually dominate the star formation rate locally (1 galaxy w/  $10^3 M_\odot/\text{yr}$  =  $10^3$  galaxies w/  $1 M_\odot/\text{yr}$ )

## ULIRGs have extremely high gas surface densities ( $10^2$ - $10^5 M_\odot/\text{pc}^2$ within $R < 0.1$ - $1$ kpc)

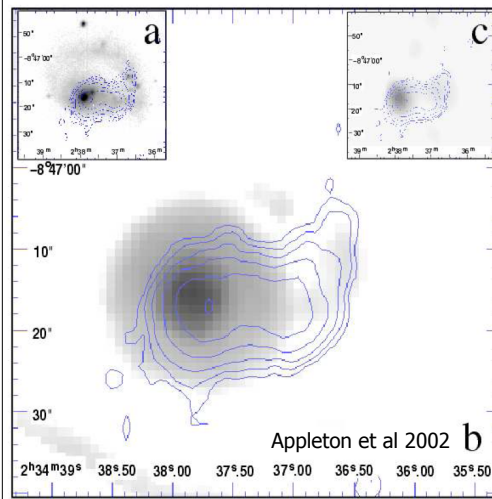
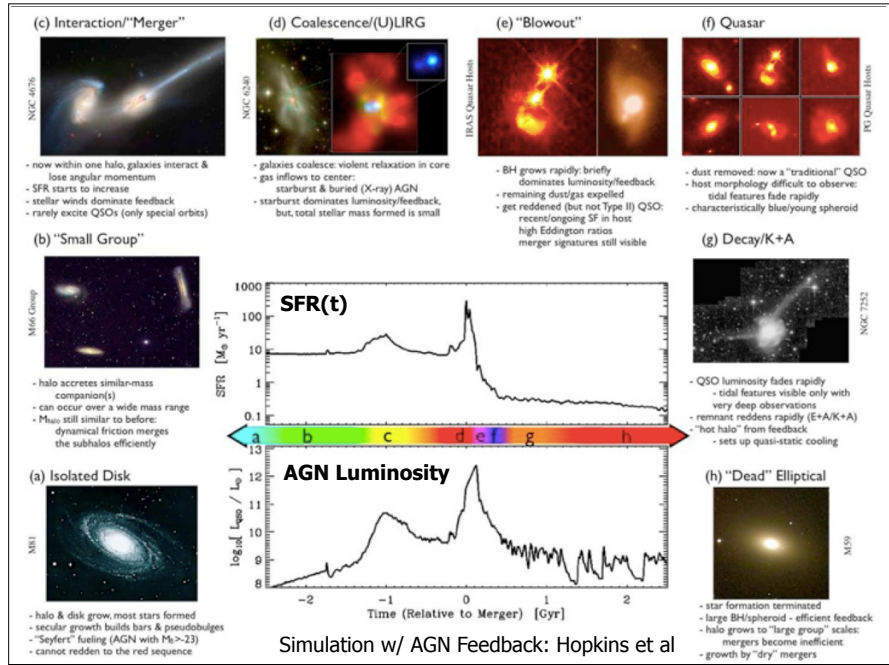
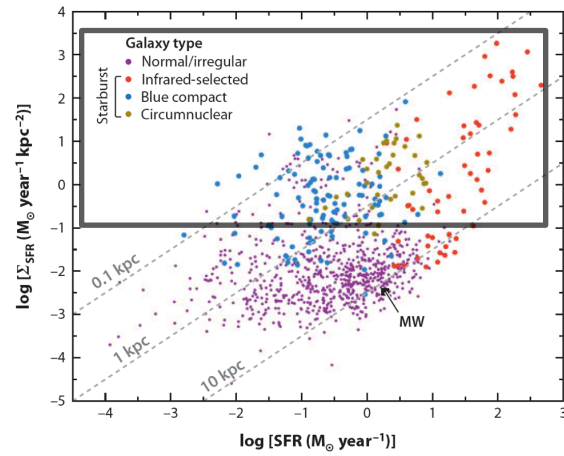


FIG. 5.— a) The integrated  $^{12}\text{CO}(1-0)$  emission in contours, over the optical R-band image of NGC 985. The contour levels are 4.0, 5.2, 6.8, 8.8, 11.5 and 15.0 Jy beam $^{-1}$  km s $^{-1}$ . b) Same as in a) but the background is the 15  $\mu\text{m}$  image of the galaxy. c) Same as in a) but the background is the 3.5 cm (X-band) radio continuum map.

- Equivalent to a galaxy's whole ISM funnelled into the center.
- Possibly associated with AGN activity (lots of gas dumping onto central BH)
- SFR is near maximum possible ( $\text{SFR}_{\text{max}} \sim M_{\text{gas}}/t_{\text{dyn}}$ )



## The High SFR End



Possible Definitions of "High"

- High absolute SFRs
- High SFR intensities
- High SFRs compared to past average

94

## Blue Compact Dwarfs (BCDs)



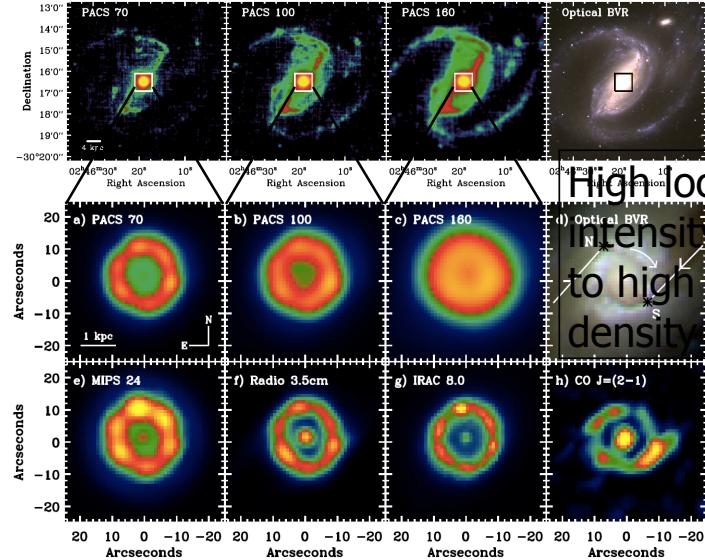
I Zw 18

95

- Very high SFR intensity
- Very low mass
- Among lowest metallicity galaxies known

Well represented in Zwicky catalog, Markarian catalog

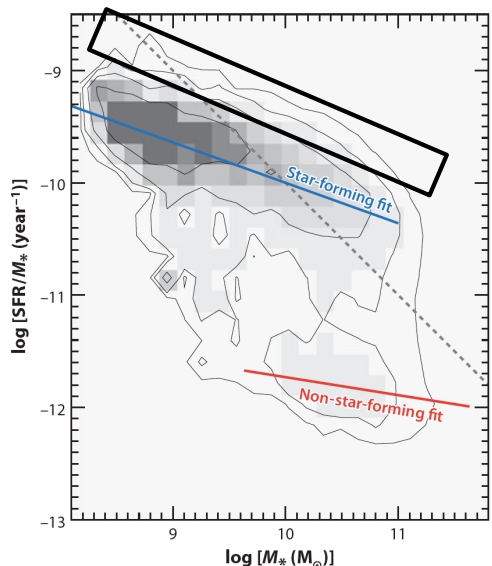
## Nuclear Star Forming Regions



Sandstrom et al 2010

96

## The High SFR End



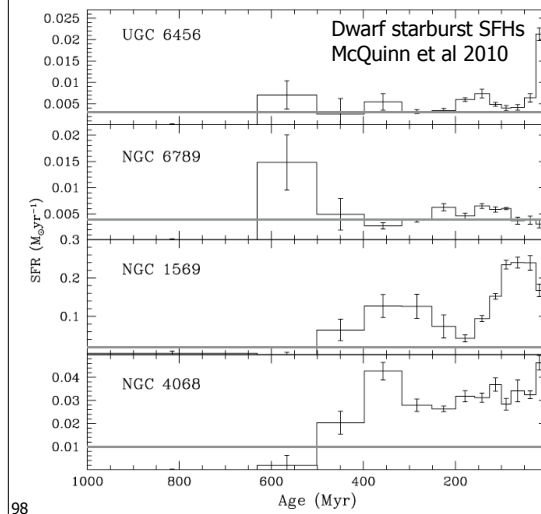
Possible Definitions of "High"

High absolute SFRs

High SFR intensities

High SFRs compared to past average

## Starbursts: Usually defined as >2-3 times past average SFR



Possible Triggers?

Interactions?

Gas accretion?